The Canadian Mineralogist
Vol. 42, pp. 973-996 (2004)

MONOVALENT CATIONS IN STRUCTURES OF THE META-AUTUNITE GROUP

ANDREW J. LOCOCK[§] AND PETER C. BURNS

Department of Civil Engineering and Geological Sciences, University of Notre Dame, 156 Fitzpatrick Hall, Notre Dame, Indiana 46556, U.S.A.

M. JOHN M. DUKE

SLOWPOKE Nuclear Reactor Facility, 3118 Dentistry-Pharmacy Building, University of Alberta, Edmonton, Alberta T6G 2E3, Canada

THEODORE M. FLYNN

Department of Civil Engineering and Geological Sciences, University of Notre Dame, 156 Fitzpatrick Hall, Notre Dame, Indiana 46556, U.S.A.

ABSTRACT

Compounds of the meta-autunite group containing monovalent cations (Li, Na, K, Rb, Cs, Ag, Tl) have been synthesized by diffusion in gels or by hydrothermal methods, and their crystal structures determined. Single-crystal X-ray-diffraction intensity data were collected at room temperature using Mo$K\alpha$ radiation and a CCD-based area detector. These compounds contain the autunite-type sheet with composition $[(UO_2)(XO_4)]^-$, X = P or As, which involves the sharing of equatorial vertices of uranyl square bipyramids with tetrahedra. The interlayer region contains cations and H_2O groups, and the sheets are linked by hydrogen bonding and through bonds from the interlayer cations to oxygen atoms of the sheets. The structural roles of the interlayer cations in determining the symmetries and hydration states observed are discussed. The smallest monovalent cation, Li, occurs in tetrahedral coordination between fourfold squares of hydrogen-bonded H_2O groups. Despite a wide range in ionic radius, Na, K, Rb, Ag and Tl randomly substitute for H_2O groups in the interlayer, in the same fashion as their ammonium and oxonium analogues. The large Cs cation adopts independent crystallographic sites in the interlayer. The size difference between Cs and the other monovalent cations probably prevents their direct substitution, and may limit the extent of solid solution. With the exception of the Rb and Cs compounds, chemically corresponding uranyl phosphates and uranyl arsenates are isostructural. The structural similarity of $Rb[(UO_2)(AsO_4)](H_2O)_3$ with metazeunerite, $Cu[(UO_2)(AsO_4)]_2(H_2O)_8$, may indicate a mechanism of solid solution for monovalent and divalent interlayer cations in the meta-autunite group. Crystallographic data: $Li[(UO_2)(PO_4)](H_2O)_4$: tetragonal, *P*4/*n*, *a* 6.9555(2), *c* 9.1389(3) Å, *R*1 = 1.2%; $Na[(UO_2)(PO_4)](H_2O)_3$: tetragonal, *P*4/*ncc*, *a* 6.9616(2), *c* 17.2677(9) Å, *R*1 = 2.3%; $Na[(UO_2)(AsO_4)](H_2O)_3$: tetragonal, *P*4/*ncc*, *a* 7.1504(3), *c* 17.325(1) Å, *R*1 = 1.7%; $K[(UO_2)(AsO_4)](H_2O)_3$: tetragonal, *P*4/*ncc*, *a* 7.1669(17), *c* 17.867(6) Å, *R*1 = 3.4%; $Rb[(UO_2)(PO_4)](H_2O)_3$: tetragonal, *P*4/*ncc*, *a* 7.0106(2), *c* 17.9772(8) Å, *R*1 = 2.6%; $Rb[(UO_2)(AsO_4)](H_2O)_3$: tetragonal, *P*4/*n*, *a* 7.1904(3), *c* 17.643(1) Å, *R*1 = 1.9%; $Ag[(UO_2)(PO_4)](H_2O)_3$: tetragonal, *P*4/*ncc*, *a* 6.9332(1), *c* 16.9313(6) Å, *R*1 = 1.6%; $Ag[(UO_2)(AsO_4)](H_2O)_3$: tetragonal, *P*4/*ncc*, *a* 7.0901(2), *c* 17.0453 (8) Å, *R*1 = 2.1%; $Tl[(UO_2)(PO_4)](H_2O)_3$: tetragonal, *P*4/*ncc*, *a* 7.019(3), *c* 17.98(1) Å, *R*1 = 3.2%; $Tl[(UO_2)(AsO_4)](H_2O)_3$: tetragonal, *P*4/*ncc*, *a* 7.1905(8), *c* 17.970(3) Å, *R*1 = 3.4%; $Cs_2[(UO_2)(PO_4)]_2(H_2O)_5$: monoclinic, $P2_1/n$, *a* 9.8716(7), *b* 9.9550(7), *c* 17.6465(13) Å, β = 90.402(2)°, *R*1 = 2.8%; $Cs(H_3O)[(UO_2)(AsO_4)]_2(H_2O)_5$: monoclinic, $P2_1/n$, *a* 14.2614(17), *b* 7.1428(9), *c* 17.221(2) Å, β 91.110(3)°, *R*1 = 4.6%.

Keywords: chernikovite, trögerite, abernathyite, meta-ankoleite, sodium meta-autunite, sodium uranospinite, uranyl phosphate, uranyl arsenate, oxonium, meta-autunite group, crystal structure.

SOMMAIRE

Nous avons synthétisé les composés du groupe de la méta-autunite contenant des cations monovalents (Li, Na, K, Rb, Cs, Ag, Tl) par diffusion dans des gels ou bien par voie hydrothermale, et nous en avons caractérisé leur structure cristalline. Les données sur l'intensité des réflexions en diffraction X ont été prélevées sur monocristaux à température ambiante avec un rayonnement Mo$K\alpha$ et un détecteur à aire de type CCD. Ces composés contiennent un feuillet de type autunite avec une composition

§ *E-mail address*: alocock@nd.edu

$[(UO_2)(XO_4)]^-$, X = P ou As, qui implique un partage des coins équatoriaux des bipyramides carrées à uranyle avec les tétraèdres. La région interfoliaire contient des cations et des groupes H_2O, et les feuillets sont interliés par liaisons hydrogène et par liaisons entre les cations et les atomes d'oxygène faisant partie des feuillets. Les cations interfoliaires exercent un rôle déterminant dans la symétrie et le taux d'hydratation de ces composés. Le plus petit cation monovalent, Li, adopte une coordinence tétraédrique entre les agencements carrés de groupes H_2O à liaisons hydrogène. Malgré une grande variation des rayons ioniques, Na, K, Rb, Ag et Tl substituent de façon aléatoire pour les groupes H_2O dans l'interfeuillet, de la même façon que dans les analogues à ammoniaque et oxonium. Le cation Cs, plus gros, adopte des sites indépendants cristallographiques dans l'interfeuillet. La différence en taille entre le Cs et les autres cations monovalents serait probablement une entrave à leur substitution directe, et pourrait limiter l'étendue de la solution solide. A l'exception des composés de Rb et de Cs, les phosphates et les arsenates à uranyle chimiquement correspondants sont isostructuraux. La ressemblance structurale de $Rb[(UO_2)(AsO_4)](H_2O)_3$ à la métazeunérite, $Cu[(UO_2)(AsO_4)]_2(H_2O)_8$, pourrait indiquer un mécanisme de solution solide pour impliquer une substitution entre cations monovalents et bivalents dans l'interfeuillet du groupe de la méta-autunite. Données cristallographiques: $Li[(UO_2)(PO_4)](H_2O)_4$: tétragonal, $P4/n$, a 6.9555(2), c 9.1389(3) Å, $R1$ = 1.2%; $Na[(UO_2)(PO_4)](H_2O)_3$: tétragonal, $P4/ncc$, a 6.9616(2), c 17.2677(9) Å, $R1$ = 2.3%; $Na[(UO_2)(AsO_4)](H_2O)_3$: tétragonal, $P4/ncc$, a 7.1504(3), c 17.325(1) Å, $R1$ = 1.7%; $K[(UO_2)(AsO_4)](H_2O)_3$: tétragonal, $P4/ncc$, a 7.1669(17), c 17.867(6) Å, $R1$ = 3.4%; $Rb[(UO_2)(PO_4)](H_2O)_3$: tétragonal, $P4/ncc$, a 7.0106(2), c 17.9772(8) Å, $R1$ = 2.6%; $Rb[(UO_2)(AsO_4)](H_2O)_3$: tétragonal, $P4/n$, a 7.1904(3), c 17.643(1) Å, $R1$ = 1.9%; $Ag[(UO_2)(PO_4)](H_2O)_3$: tétragonal, $P4/ncc$, a 6.9332(1), c 16.9313(6) Å, $R1$ = 1.6%; $Ag[(UO_2)(AsO_4)](H_2O)_3$: tétragonal, $P4/ncc$, a 7.0901(2), c 17.0453 (8) Å, $R1$ = 2.1%; $Tl[(UO_2)(PO_4)](H_2O)_3$: tétragonal, $P4/ncc$, a 7.019(3), c 17.98(1) Å, $R1$ = 3.2%; $Tl[(UO_2)(AsO_4)](H_2O)_3$: tétragonal, $P4/ncc$, a 7.1905(8), c 17.970(3) Å, $R1$ = 3.4%; $Cs_2[(UO_2)(PO_4)]_2(H_2O)_5$: monoclinique, $P2_1/n$, a 9.8716(7), b 9.9550(7), c 17.6465(13) Å, β = 90.402(2)°, $R1$ = 2.8%; $Cs(H_3O)[(UO_2)(AsO_4)]_2(H_2O)_5$: monoclinique, $P2_1/n$, a 14.2614(17), b 7.1428(9), c 17.221(2) Å, β 91.110(3)°, $R1$ = 4.6%.

(Traduit par la Rédaction)

Mots-clés: chernikovite, trögerite, abernathyite, méta-ankoléite, sodium méta-autunite, sodium uranospinite, phosphate à uranyle, arsenate à uranyle, oxonium, groupe de la méta-autunite, structure cristalline.

Introduction

The autunite and meta-autunite groups comprise one of the two major divisions of uranyl phosphate and uranyl arsenate minerals (the phosphuranylite group being the other), and together consist of approximately forty mineral species, of which ten have had their structures determined (Smith 1984, Finch & Murakami 1999, Burns 1999). The structures, chemical compositions and stabilities of uranyl phosphates have received considerable attention recently owing to their importance to the environment. They are amongst the most abundant of uranyl minerals, are widespread, have low solubilities, and affect the mobility of uranium in phosphate-bearing systems (Sowder *et al.* 1996) such as uranium deposits (Magalhães *et al.* 1985, Murakami *et al.* 1997), and soils contaminated by actinides (Buck *et al.* 1996, Roh *et al.* 2000).

Compounds of the autunite and meta-autunite groups are typified by the presence of the corrugated autunite-type sheet of composition $[(UO_2)(XO_4)]^-$, X = P, As, first described by Beintema (1938), in which hexavalent uranium occurs as part of a linear uranyl cation, $(UO_2)^{2+}$. The uranyl ion is coordinated by four additional O atoms arranged at the equatorial positions of a square bipyramid, with the uranyl ion O atoms at the apices of the bipyramid. The uranyl square bipyramids share equatorial vertices with tetrahedra (phosphate or arsenate) to form infinite sheets. In meta-autunite-group compounds, corresponding points in adjacent sheets lie directly above each other, whereas in autunite-group compounds, every second sheet is offset (by [½, ½, 0], assuming the sheets are perpendicular to [001]), to provide fewer but larger interlayer cavities (Beintema 1938). The interlayer region contains cations and H_2O groups, and the sheets are linked by hydrogen bonding and through bonds from the interlayer cations to oxygen atoms of the sheets. The symmetries of the compounds of the autunite and meta-autunite groups vary with their hydration states and the nature of the interlayer cations. This work concentrates on the compounds of the meta-autunite group that contain monovalent interlayer cations (M^+): $M[(UO_2)(XO_4)](H_2O)_n$.

Previous Studies

A considerable body of literature exists for uranyl phosphate and uranyl arsenate compounds of the meta-autunite group that contain monovalent cations or complex cations in the interlayer: Li^+, Na^+, K^+, Rb^+, Cs^+, Ag^+, Tl^+, H_3O^+, and NH_4^+. Early work on minerals of this group was reviewed by Frondel (1958), and their descriptions and localities are summarized in Anthony *et al.* (2000) and Gaines *et al.* (1997). Mineral species include chernikovite $H_3O[(UO_2)(PO_4)](H_2O)_3$, trögerite $H_3O[(UO_2)(AsO_4)](H_2O)_3$, meta-ankoleite $K[(UO_2)(PO_4)](H_2O)_3$, abernathyite $K[(UO_2)(AsO_4)](H_2O)_3$, sodium meta-autunite $Na[(UO_2)(PO_4)](H_2O)_3$, sodium uranospinite $(Na,Ca_{0.5})[(UO_2)(AsO_4)](H_2O)_{2.5–3(?)}$, and uramphite $NH_4[(UO_2)(PO_4)](H_2O)_3$. Further synthetic compounds of this group include Li^+, Rb^+, Cs^+, Ag^+, and Tl^+ end-members. Methods of synthesis have been presented by many investigators, including Fairchild (1929), Ross (1955), Weigel & Hoffmann (1976a),

Chernorukov *et al.* (1994a, b), Van Haverbeke *et al.* (1996), and Wellman & Icenhower (2002). Optical properties are listed by Ross (1955), Schulte (1965) and Walenta (1965). Solubility products are reported by Veselý *et al.* (1965), Marković *et al.* (1988), Van Haverbeke *et al.* (1996), and Chernorukov *et al.* (2003), and range from pK_{sp} = 22.6 to 26.4. Unit-cell dimensions determined using powder X-ray diffraction have been given by Schulte (1965), Walenta (1965), Weigel & Hoffmann (1976a), Marković *et al.* (1988), and Chernorukov *et al.* (1994a, b). Thermodynamic properties have been investigated mainly by Chernorukov and coworkers (Karyakin *et al.* 1999, Chernorukov *et al.* 2001, Suleimanov *et al.* 2002a, b).

Some bacteria can precipitate compounds of the meta-autunite group, for example chernikovite, uramphite, and sodium meta-autunite (Macaskie *et al.* 1992, 2000, and references therein). Bioprecipitation of uranyl phosphates has been suggested as a means of remediation of radionuclide contamination (Renninger *et al*. 2001).

In addition to the uranyl ion, the actinide elements Np, Pu, and Am also form hexavalent ions with the dioxo configuration yielding neptunyl $(NpO_2)^{2+}$, plutonyl $(PuO_2)^{2+}$ and americyl $(AmO_2)^{2+}$ ions (Cotton *et al.* 1999). Compounds of the meta-autunite group have been synthesized with these actinyl ions, as well as the variants derived by replacement of P with As and the various interlayer substitutions of the monovalent cations (Weigel & Hoffmann 1976b, 1976c, Fischer *et al.* 1981). The meta-autunite-group compounds of the higher actinides have been characterized mainly by powder X-ray diffraction.

The monovalent meta-autunite compounds are of interest also because of their cationic conductivity. Chernikovite and trögerite are fast proton conductors at room temperature (Childs *et al.* 1978), with alternating current conductivities of 0.3–0.6 ohm^{-1} m^{-1} (Childs *et al.* 1980, Johnson *et al.* 1981). The high conductivity in these two compounds is attributable to the presence of oxonium, H_3O^+ (Leigh 1990), and prompted studies of the mechanisms of conduction, phase transitions and thermal behavior of many of the monovalent meta-autunite-group compounds (Johnson *et al.* 1981, Pham-Thi *et al.* 1985, Pham-Thi & Colomban 1985, Metcalfe *et al.* 1988, Poinsignon 1989, Candea *et al.* 1993, Lupu *et al.* 1993). The mechanisms of conduction for the oxonium members are reviewed in Kreuer (1996) and Casciola (1996). The room-temperature alternating-current conductivities of the monovalent uranyl phosphate meta-autunite compounds with normal hydration states range over three orders of magnitude in the order H_3O^+ 0.3–0.6, Na^+ 0.01–0.02, K^+ 0.0005–0.0007, Ag^+ 0.0004, NH_4^+ 0.0002, and Li^+ 0.0001–0.0002 ohm^{-1} m^{-1} (Johnson *et al.* 1981, Pham-Thi & Colomban 1985).

At or below room temperature, the oxonium and potassium members of the meta-autunite group undergo a phase transition to lower symmetry; in the cases of the oxonium members, the lower-symmetry structures have much lower conductivities (de Benyacar & de Abeledo 1974, de Benyacar & Dussel 1975, 1978, Dussel *et al.* 1982, Pham-Thi & Colomban 1985, Shilton & Howe 1979).

Crystal structures of the monovalent members of the meta-autunite group have been reported for the K^+, NH_4^+, H_3O^+ uranyl phosphates and uranyl arsenates, and for $Li[(UO_2)(AsO_4)](H_2O)_4$; their cell dimensions and space groups are listed in Table 1. The replacement of P by As in monovalent meta-autunite structures generally entails expansion of the unit cell; the tetragonal uranyl arsenates average ~0.15 Å greater along *a*, and ~0.1 Å greater along *c*, than their chemically corresponding isostructural uranyl phosphates (Schulte 1965, Weigel & Hoffmann 1976a, Chernorukov *et al.* 1994a, b). This relationship holds true for the structures listed in Table 1 with the exception of the K members, in which the arsenate cell is larger than that of the phosphate by 0.34 Å along *c*. The literature shows good agreement for the *c* cell dimension reported from powder X-ray-diffraction data for synthetic meta-ankoleite, $K[(UO_2)(PO_4)](H_2O)_3$, 17.81 Å (Schulte 1965, Weigel & Hoffmann 1976a, Marković *et al.* 1988, Chernorukov *et al.* 1994a). However, the *c* cell dimensions reported from powder X-ray-diffraction data for synthetic abernathyite, $K[(UO_2)(AsO_4)](H_2O)_3$, range from 17.846(6) Å (Schulte 1965) to 18.14(4) Å (Chernorukov *et al.* 1994b). Although the structure has been previously refined (Ross & Evans 1964), the uncertainty in the *c* cell dimension of abernathyite prompted us to carry out a new crystal-structure refinement of this compound.

In addition to synthetic abernathyite, we have examined Li, Na, Rb, Ag, Tl, and Cs members of the meta-autunite group in order to elucidate the roles of the interlayer cations in this structure type. For simplicity, the compounds investigated are subsequently referred to by abbreviations rather than mineral names or chemi-

TABLE 1. CELL PARAMETERS OF META-AUTUNITE GROUP COMPOUNDS THAT CONTAIN MONOVALENT CATIONS

Formula	Space Group	*a* (Å)	*c* (Å)	Mineral	Ref.
$Li[(UO_2)(AsO_4)](H_2O)_4$	*P4/n*	7.097	9.190		1
$H_3O[(UO_2)(PO_4)](H_2O)_3$	*P4/ncc*	6.995	17.491	chernikovite	2
$H_3O[(UO_2)(AsO_4)](H_2O)_3$[1]	*P4/ncc*	7.162	17.639	trögerite	3
$K[(UO_2)(PO_4)](H_2O)_3$[2]	*P4/ncc*	6.994	17.784	meta-ankoleite	4
$K[(UO_2)(AsO_4)](H_2O)_3$	*P4/ncc*	7.176	18.126	abernathyite	5
$K(H_3O)[(UO_2)(AsO_4)]_2(H_2O)_6$	*P4/ncc*	7.171	18.048		5
$NH_4[(UO_2)(PO_4)](H_2O)_3$	*P4/ncc*	7.03	18.09	uramphite	6
$NH_4[(UO_2)(PO_4)](H_2O)_3$	*P4/ncc*	7.022	18.091	uramphite	7
$NH_4[(UO_2)(AsO_4)](H_2O)_3$	*P4/ncc*	7.189	18.191		5

[1] At 4 K: *P*-1, *a* 7.164 Å, *b* 7.112 Å, *c* 17.554 Å, α 90.19°, β 89.95°, γ 90.00° (Fitch *et al.* 1982b). [2] At 10 K: $P2_1cn$, *a* 6.993 Å, *b* 6.973 Å, *c* 17.611 Å (Cole *et al.* 1993). References: (1) Fitch *et al.* (1982a), (2) Morosin (1978a,b), (3) Fitch *et al.* (1983), (4) Fitch & Cole (1991), (5) Ross & Evans (1964), (6) Botto *et al.* (1975), (7) Fitch & Fender (1983).

cal formulas: *LiUP* = $Li[(UO_2)(PO_4)](H_2O)_4$; *NaUP* = $Na[(UO_2)(PO_4)](H_2O)_3$; *NaUAs* = $Na[(UO_2)(AsO_4)](H_2O)_3$; *KUAs* = $K[(UO_2)(AsO_4)](H_2O)_3$; *RbUP* = $Rb[(UO_2)(PO_4)](H_2O)_3$; *RbUAs* = $Rb[(UO_2)(AsO_4)](H_2O)_3$; *AgUP* = $Ag[(UO_2)(PO_4)](H_2O)_3$; *AgUAs* = $Ag[(UO_2)(AsO_4)](H_2O)_3$; *TlUP* = $Tl[(UO_2)(PO_4)](H_2O)_3$; *TlUAs* = $Tl[(UO_2)(AsO_4)](H_2O)_3$; *CsUP* = $Cs_2[(UO_2)(PO_4)]_2(H_2O)_5$; *CsHUAs* = $Cs(H_3O)[(UO_2)(AsO_4)]_2(H_2O)_5$.

Experimental

Synthesis

The interlayer contents of compounds of the autunite and meta-autunite groups are easily exchangeable, and intercalation of cations into previously crystallized material, generally $H_3O[(UO_2)(PO_4)](H_2O)_3$, has been a common method of synthesis (*e.g.*, Fairchild 1929, Garcia & Diaz 1959a, b, 1962, Dieckmann & Ellis 1987, Vochten 1990, Benavente *et al.* 1995). However, this method does not yield single crystals; the mosaic spread, as determined by X-ray diffraction, within the ion-exchanged crystals is rather more consistent with a powder sample. In order to obtain single crystals of good quality, direct means of crystal synthesis were employed in this work.

Crystals of nine of the compounds (Table 2) were grown at room temperature over weeks to months by slow diffusion of phosphoric acid or hydrogen arsenate, and uranyl nitrate into cation-bearing silica gels contained in U-shaped tubes (Fig. 1). The gels were formed by the hydrolysis of a mixture of tetramethoxysilane (TMOS) and aqueous solutions of metal nitrates or metal chlorides (Table 2). This method was modified after: Arend & Connelly (1982), Manghi & Polla (1983), Zolensky (1983), Perrino & LeMaster (1984), Robert & LeFaucheux (1988), and Henisch (1988). Crystals of *KUAs*, *AgUAs* and *TlUAs* were obtained by hydrothermal synthesis (Table 3), in which the reactants were weighed into 23 mL Teflon-lined Parr acid-digestion vessels and heated in Fisher Isotemp ovens.

Instrumental neutron-activation analysis

The compounds investigated were synthesized in systems of restricted composition. During crystal-structure refinement, the identities (and proportions) of the interlayer cations can be distinguished unambiguously from H_2O groups by their differing scattering powers

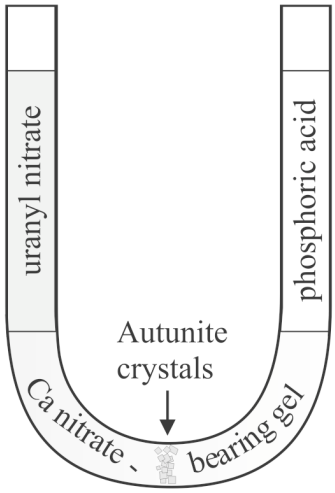

Fig. 1. Growth of autunite by the method of diffusion in a gel.

TABLE 2. SYNTHESES BY DIFFUSION-IN-GEL METHODS

Compound	*LiUP*	*NaUP*	*NaUAs*	*RbUP*	*RbUAs*
Gel	TMOS	TMOS	TMOS	TMOS	TMOS
	1.0 M $LiNO_3$	2.9 M $NaNO_3$	2.9 M $NaNO_3$	0.2 M $RbNO_3$	0.2 M RbCl
Left arm	0.1 M uranyl nitrate	0.08 M uranyl nitrate	0.08 M uranyl nitrate	0.1 M uranyl nitrate	0.1 M uranyl nitrate
					0.2 M RbCl
Right arm	0.1 M H_3PO_4	0.1 M H_3PO_4	0.033 M $H_5As_3O_{10}$	0.1 M H_3PO_4	0.033 M $H_5As_3O_{10}$
					0.2 M RbCl
Time	2 weeks	3 weeks	3 weeks	3 months	1 month

Compound	*AgUP*	*TlUP*	*CsUP*	*CsHUAs*
Gel	TMOS	TMOS	TMOS	TMOS
	0.2 M $AgNO_3$	0.2 M $TlNO_3$	0.3 M $CsNO_3$	0.2 M CsCl
Left arm	0.1 M uranyl nitrate	0.1 M uranyl nitrate	0.1 M uranyl nitrate	0.1 M uranyl nitrate
			0.3 M $CsNO_3$	0.2 M CsCl
Right arm	0.1 M H_3PO_4	0.1 M H_3PO_4	0.1 M H_3PO_4	0.033 M $H_5As_3O_{10}$
			0.3 M $CsNO_3$	0.2 M CsCl
Time	1 month	2 weeks	3 weeks	6 months

Note: gel volumes are 11 mL (1 mL TMOS + 10 mL aqueous solution); arm volumes are 6 mL each. All solutions are aqueous. TMOS = tetramethoxysilane, $(CH_3O)_4Si$.

TABLE 3. HYDROTHERMAL SYNTHESES

Compound	*KUAs*	*AgUAs*	*TlUAs*
Reagents	0.2756 g KNO_3	0.2195 g $AgNO_3$	0.3413 g $TlNO_3$
	0.1013 g $UO_2(NO_3)_2(H_2O)_6$	0.1121 g $UO_2(NO_3)_2(H_2O)_6$	0.1073 g $UO_2(NO_3)_2(H_2O)_6$
	0.0653 g $H_5As_3O_{10}$	0.0603 g $H_5As_3O_{10}$	0.0614 g $H_5As_3O_{10}$
	4.03 g H_2O	4.15 g H_2O	4.38 g H_2O
Temperature	180°C	190°C	190°C
Time	7 days	6 days	6 days

(Hawthorne *et al.* 1995), with the exception of Na, whose behavior in these structures is anomalous. Electron-microprobe methods would normally be used to assess the Na content of the synthesized crystals. However, Butt & Graham (1981) and Graham *et al.* (1984) found that the beam-induced mobility of Na in sodium meta-autunite is so high that electron-microprobe analysis cannot be used. For example, in a natural specimen, the Na count-rate approached background within 3 s under normal operating conditions.

Because of the insufficiency of both single-crystal structure refinement and electron-microprobe analysis to measure the Na content of *NaUP* and *NaUAs*, instrumental neutron-activation analysis (INAA) was carried out instead using the SLOWPOKE nuclear reactor facility at the University of Alberta. Samples of *NaUP* and *NaUAs* were removed from their gel-growth medium, washed with ultrapure H_2O and dried at 60°C. In order to allay concerns about self-shielding, samples (*NaUP* 3.59 mg, *NaUAs* 3.22 mg) were weighed into 7 mL Savellex screw top beakers and completely dissolved in 100 μL of Analar 15.8 M HNO_3. Following dissolution, the samples were made up to a total volume of 4.10 mL by the addition of 4.00 mL of Millipore water (18.5 MΩ/cm resistivity), giving a *ca.* 2.5% HNO_3 solution. After vigorous mixing, 250 μL aliquots of each sample were pipetted into 300 μL polyethylene microcentrifuge tubes that were then trimmed and hermetically sealed. Comparator standards for the determination of As, U and Na, were prepared from a mixed-element SCP Science PlasmaCAL trace-metals standard with an As concentration of 100.9 μg/mL (Lot # SC3098203), an aqueous U standard made from Alfa Aesar U metal turnings (99.7% pure, Stock No. 39692, Lot # G18L26), and an aqueous Na standard prepared from Aldrich Chemicals sodium carbonate (99.999% pure) that was dried and cooled prior to standard preparation. As with the 250 μL samples, an aliquot of each standard was pipetted into a 300 μL polyethylene microcentrifuge tube that was immediately trimmed and hermetically sealed. Samples and standards were irradiated as a batch, together with a blank vial with 250 μL of Millipore water, for 900 s (15 minutes) in an inner irradiation site of the University of Alberta SLOWPOKE nuclear reactor at a nominal thermal neutron flux of 5×10^{11} n cm^{-2} s^{-1}. Following a minimum decay of 4 hours (to permit the complete decay of ^{239}U to ^{239}Np), samples and standards were individually counted at a sample-to-detector distance of 3 cm using a 41% hyperpure Ge detector. Counting times for samples and standards varied from ~15 minutes to 1 hour. The amount of uranium was quantified *via* ^{239}Np ($T_{½}$ = 2.3565 d), arsenic *via* ^{76}As ($T_{½}$ = 1.0778 d), and sodium *via* ^{24}Na ($T_{½}$ = 14.959 h). The determination of uranium was made using the gamma-ray emissions at 277.8, 228.2, 316.3 and 334.7 keV, whereas As and Na were determined using gamma-ray emissions at 559.1 keV and 1368.4 keV, respectively. Neutron activation of monoisotopic phosphorus produces ^{32}P *via* the nuclear reaction $^{31}P(n,\gamma)^{32}P$. As ^{32}P is a pure beta emitter and emits no gamma rays, its concentration was not determined in this study. Elemental analysis was performed by the semi-absolute method of activation analysis (Bergerioux *et al.* 1979).

The INAA results for U, As and Na are within 2σ of the experimental uncertainty of the expected elemental contents of the end-member compounds, *NaUP*: measured U = 54.0(5) wt% (expected U = 53.85 wt%), measured Na = 5.0(2) wt% (expected Na = 5.20 wt%); *NaUAs*: measured U = 48.7(8) wt% (expected U = 48.98 wt%), measured As = 15.8(2) wt% (expected As = 15.42 wt%), measured Na = 5.1(2) wt% (expected Na = 4.73 wt%). The Na contents determined by INAA are consistent with maximum Na occupancy in the structures of *NaUP* and *NaUAs*.

Single-crystal X-ray diffraction

For each of the twelve compounds, a suitable crystal was mounted on a Bruker PLATFORM three-circle X-ray diffractometer operated at 50 keV and 40 mA, equipped with a 4K APEX CCD detector and a crystal-to-detector distance of ~4.7 cm. Data were collected at room temperature using graphite-monochromatized Mo*K*α X-radiation and frame widths of 0.3° in ω. Details of the data acquisition and refinement parameters are provided in Table 4. The intensity data were reduced and corrected for Lorentz, polarization, and background effects using the program SAINT (Bruker 1998), and the unit-cell dimensions were refined using least-squares techniques.

TABLE 4. CRYSTALLOGRAPHIC DATA AND REFINEMENT PARAMETERS

Compound	$Li[(UO_2)(PO_4)](H_2O)_4$	$Na[(UO_2)(PO_4)](H_2O)_3$	$Na[(UO_2)(AsO_4)](H_2O)_3$	$K[(UO_2)(AsO_4)](H_2O)_3$	$Rb[(UO_2)(PO_4)](H_2O)_3$	$Rb[(UO_2)(AsO_4)](H_2O)_3$
a (Å)	6.9555(2)	6.9616(2)	7.1504(3)	7.1669(17)	7.0106(2)	7.1904(3)
b (Å)						
c (Å)	9.1389(3)	17.2677(9)	17.325(1)	17.867(6)	17.9772(8)	17.643(1)
β (°)	90	90	90	90	90	90
V (Å^3)	442.13	836.86	885.78	917.73	883.55	912.19
Space group	*P4/n*	*P4/ncc*	*P4/ncc*	*P4/ncc*	*P4/ncc*	*P4/n*
Z	2	4	4	4	4	4
Formula weight[1]	444.001	442.035	485.983	502.091	504.513	548.461
$F(000)$[1]	396	784	856	888	888	960
μ (mm^{-1})[1]	18.57	19.66	22.10	21.73	24.04	26.71
D_{calc} (g/mL)[1]	3.335	3.508	3.644	3.634	3.793	3.994
Size (mm)	0.28 x 0.28 x 0.02	0.20 x 0.20 x 0.03	0.10 x 0.10 x 0.01	0.40 x 0.28 x 0.015	0.30 x 0.30 x 0.04	0.15 x 0.15 x 0.02
Color and habit	yellow plate	yellow plate	yellow plate	yellow plate	yellow plate	yellow plate
Temperature (K)	293(2)	293(2)	293(2)	293(2)	293(2)	293(2)
Width (°), time (s)	0.3, 5	0.3, 10	0.3, 40	0.3, 10	0.3, 20	0.3, 10
Collection, hours	sphere, 4	sphere, 8	sphere, 30	sphere, 8	sphere, 16	sphere, 8
θ range (°)	2.9 – 34.5	3.8 – 34.5	3.7 – 34.4	3.6 – 34.5	3.7 – 34.5	2.8 – 34.5
Data collected	h±11, k±10, l±14	-11≤h≤10, k±10, -26≤l≤27	h±11, k±11, -27≤l≤24	h±11, k±11, -28≤l≤27	h±10, k±10, l±27	h±11, k±11, l±27
Absorption[2]	plate (001) 3°	plate (001) 3°	plate (001) 3°	plate (001) 3°	plate (001) 3°	face-indexed
Total refl.	8128	13373	12086	14941	13825	16336
Unique refl., R_{int}	933, 0.052	888, 0.045	941, 0.048	977, 0.110	928, 0.090	1944, 0.092
Unique $\lvert F_o\rvert \geq 4\sigma_F$	912	605	580	726	758	1063
Extinction					0.0034(3)	0.00022(6)
Twin matrix	[010/100/00-1]					[010/100/00-1]
Twin proportion (%)	27.9(2)					14.6(2)
Parameters	39	30	30	31	32	62
$R1$[3] for $\lvert F_o\rvert \geq 4\sigma_F$	1.2	2.3	1.7	3.4	2.6	1.9
$R1$[3] all data, wR_2[4]	1.3, 2.6	3.5, 5.9	3.6, 4.1	5.0, 7.9	3.3, 6.3	5.5, 3.7
Weighting *a, b*	0.0091	0.0318, 0.492	0.185	0.0277, 1.74	0.0230, 3.10	0.0
Goodness of fit	1.060	1.097	0.885	1.287	1.157	0.754
Mean shift/esd	0.000	0.000	0.000	0.000	0.000	0.000
Peaks (e/Å^3)	0.6, -1.2	4.5, -0.7	3.2, -0.8	4.4, -1.7	2.1, -1.5	1.5, -0.9

[1] Calculated with ideal occupancy of all atomic positions. [2] Corrections for absorption are either semi-empirical (crystal modelled as a plate, rejecting data within 3° of the primary X-ray beam), face-indexed analytical, or empirical (program SADABS, G. Sheldrick, unpublished) based on the intensities of equivalent reflections. [3] $R1 = [\Sigma\lvert\lvert F_o\rvert - \lvert F_c\rvert\rvert]/\Sigma\lvert F_o\rvert$ x 100. [4] $wR_2 = [\Sigma[w(F_o^2 - F_c^2)^2]/\Sigma[w(F_o^2)^2]]^{0.5}$ x 100, $w = 1/(\sigma^2(F_o^2) + (a \cdot P)^2 + b \cdot P)$, and $P = 1/3 \max(0, F_o^2) + 2/3 F_c^2$.

TABLE 4. CRYSTALLOGRAPHIC DATA AND REFINEMENT PARAMETERS (CONTINUED)

Compound	$Ag[(UO_2)(PO_4)](H_2O)_3$	$Ag[(UO_2)(AsO_4)](H_2O)_3$	$Tl[(UO_2)(PO_4)](H_2O)_3$	$Tl[(UO_2)(AsO_4)](H_2O)_3$	$Cs_2[(UO_2)(PO_4)]_2(H_2O)_5$	$Cs(H_3O)[(UO_2)(AsO_4)]_2(H_2O)_5$
a (Å)	6.9332(1)	7.0901(2)	7.019(3)	7.1905(8)	9.8716(7)	14.2614(17)
b (Å)					9.9550(7)	7.1428(9)
c (Å)	16.9313(6)	17.0453 (8)	17.98(1)	17.970(3)	17.6465(13)	17.221(2)
β (°)	90	90	90	90	90.402(2)	91.110(3)
V (Å^3)	813.88	856.86	885.76	929.09	1734.11	1753.94
Space group	*P4/ncc*	*P4/ncc*	*P4/ncc*	*P4/ncc*	$P2_1/n$	$P2_1/n$
Z	4	4	4	4	4	4
Formula weight [1]	526.913	570.861	623.428	667.376	1085.885	1059.899
$F(000)$ [1]	928	1000	1064	1136	1880	1848
μ (mm^{-1}) [1]	22.49	25.01	36.63	38.28	23.05	24.31
D_{calc} (g/mL) [1]	4.300	4.425	4.675	4.771	4.159	4.014
Size (mm)	0.20 x 0.15 x 0.015	0.30 x 0.20 x 0.01	0.20 x 0.20 x 0.01	0.10 x 0.10 x 0.01	0.08 x 0.08 x 0.01	0.10 x 0.05 x 0.01
Color and habit	yellow plate	yellow plate	yellow plate	yellow plate	yellow plate	yellow plate
Temperature (K)	293(2)	293(2)	293(2)	293(2)	293(2)	293(2)
Width (°), time (s)	0.3, 20	0.3, 10	0.3, 20	0.3, 30	0.3, 30	0.3, 25
Collection, hours	sphere, 16	sphere, 8	sphere, 16	hemisphere, 12	sphere, 23	sphere, 18
θ range (°)	3.8 – 34.5	3.7 – 34.5	3.7 – 34.5	3.6 – 34.5	2.0 – 34.5	1.4 – 34.5
Data collected	h±11, k±10, l±26	h±11, k±11, l±26	-10≤h≤11, k±11, l±28	-6≤h≤11, k±11, -28≤l≤27	h±15, k±15, l±27	h±22, k±11, l±26
Absorption [2]	plate (001) 3°	plate (001) 3°	plate (001) 3°	plate (001) 3°	plate (001) 3°	SADABS
Total refl.	13027	13800	14092	8308	32274	36041
Unique refl., R_{int}	869, 0.050	907, 0.052	946, 0.294	990, 0.148	7193, 0.064	7238, 0.078
Unique $\lvert F_o\rvert \geq 4\sigma_F$	673	645	666	683	3250	2780
Extinction	0.00075(18)					
Twin matrix					[100/0-10/00-1]	[100/0-10/00-1]
Twin proportion (%)					0.26(5)	3.0(2)
Parameters	32	31	31	31	209	209
$R1$ [3] for $\lvert F_o\rvert \geq 4\sigma_F$	1.6	2.1	3.2	3.4	2.8	4.6
$R1$ [3] all data, wR_2 [4]	2.1, 4.6	3.2, 5.4	5.1, 7.4	5.2, 6.9	8.8, 4.8	12.8, 9.4
Weighting a, b	0.0258, 0.3488	0.0318	0.0	0.0202	0.0041	0.030
Goodness of fit	1.084	0.994	0.948	0.936	0.693	0.786
Mean shift/esd	0.000	0.000	0.000	0.000	0.000	0.000
Peaks (e/Å^3)	1.1, -0.8	2.9, -0.8	2.1, -2.0	4.3, -2.9	1.4, -1.3	5.2, -2.3

[1] Calculated with ideal occupancy of all atomic positions. [2] Corrections for absorption are either semi-empirical (crystal modelled as a plate, rejecting data within 3° of the primary X-ray beam), face-indexed analytical, or empirical (program SADABS, G. Sheldrick, unpublished) based on the intensities of equivalent reflections. [3] $R1 = [\Sigma||F_o| - |F_c||]/\Sigma|F_o|$ x 100. [4] $wR_2 = [\Sigma[w(F_o^2 - F_c^2)^2]/\Sigma[w(F_o^2)^2]]^{0.5}$ x 100, $w = 1/(\sigma^2(F_o^2) + (a \cdot P)^2 + b \cdot P)$, and $P = 1/3 \max(0, F_o^2) + 2/3 F_c^2$.

Space group *P*4/*n* was assigned to *LiUP*, by analogy with the structure refinement of $Li[(UO_2)(AsO_4)](H_2O)_4$ (Fitch *et al.* 1982a). Systematic absences of reflections for *NaUP, NaUAs, KUAs, RbUP, AgUP, AgUAs, TlUP*, and *TlUAs* are consistent with space group *P*4/*nnc* only. In contrast, systematic absences of reflections for *RbUAs* are consistent with space groups *P*4/*nmm* and *P*4/*n*; reasonable refined atomic displacement parameters were obtained only for solutions in *P*4/*n*. A solution in *P*4/*nnc* was attempted for *RbUAs*, by analogy with *RbUP*, but yielded 135 violations (intensities > 3σ) of the *c* glides, and unreasonably short interatomic distances between the Rb and O positions. Systematic absences of reflections for *CsUP* and *CsHUAs* are consistent with space group $P2_1/n$ only. The unit cells of *CsUP* and *CsHUAs* (Table 4) can be transformed to the conventional setting with space group $P2_1/c$ by the matrix $[00\bar{1}/0\bar{1}0/\bar{1}01]$; however, the resultant cells, *a* 17.646 Å, *b* 9.955 Å, *c* 20.280 Å, β 150.87°, and *a* 17.221 Å, *b* 7.143 Å, *c* 22.572 Å, β 140.82°, respectively, are quite oblique; therefore, the structures were solved in the settings with β close to 90°.

Scattering curves for neutral atoms, together with anomalous dispersion corrections, were taken from *International Tables for X-ray Crystallography, Volume IV* (Ibers & Hamilton 1974). The SHELXTL Version 5 (Sheldrick 1998) series of programs was used for the solution and refinement of the crystal structures.

Structure solution and refinement

All twelve structures were refined on the basis of F^2 for all unique data, and included anisotropic displacement parameters for all non-H atoms. In the final cycle of each refinement, the mean parameter shift/esd was 0.000.

The crystal structure of *LiUP* was refined using the non-H atomic positions of Fitch *et al.* (1982a) for $Li[(UO_2)(AsO_4)](H_2O)_4$ as a starting point. Possible positions of the H atoms were located in difference-Fourier maps, calculated following refinement of the model. Their positions were refined with the restraint that O–H bond-lengths be ~0.96 Å and with fixed isotropic displacement parameters. The refinement provided a crystallochemically reasonable network of H-bonds. Because *LiUP* was solved in a low-symmetry tetragonal space-group, the twin law $[010/100/00\bar{1}]$ was applied, the structure was refined according to published methods (Jameson 1982, Herbst-Irmer & Sheldrick 1998), and resulted in a significant improvement of the agreement index ($R1$ = 1.2%). The twin-component scale-factor refined to 27.9(2)%.

The crystal structures of *NaUP, NaUAs, KUAs, RbUP, AgUP, AgUAs, TlUP*, and *TlUAs* were refined using the atomic positions of Ross & Evans (1964) for $K[(UO_2)(AsO_4)](H_2O)_3$ as a starting point. The agreement indices ($R1$), calculated for the observed unique reflections ($|F_o| \geq 4\sigma_F$) of these refinements, range from 1.7 to 3.4% (Table 4). The location of each H atom in these structures was not determined. The site occupancies of the interlayer cations (Hawthorne *et al.* 1995) were refined in the cases of *KUAs, RbUP, AgUP, AgUAs, TlUP*, and *TlUAs* and yield the following empirical formulas: *KUAs*: $K_{0.91}(H_3O)_{0.09}[(UO_2)(AsO_4)](H_2O)_3$, *RbUP*: $Rb_{0.75}(H_3O)_{0.25}[(UO_2)(PO_4)](H_2O)_3$, *AgUP*: $Ag_{0.87}(H_3O)_{0.13}[(UO_2)(PO_4)](H_2O)_3$, *AgUAs*: $Ag_{0.93}(H_3O)_{0.07}[(UO_2)(AsO_4)](H_2O)_3$, *TlUP*: $Tl_{0.98}(H_3O)_{0.02}[(UO_2)(PO_4)](H_2O)_3$, *TlUAs*: $Tl[(UO_2)(AsO_4)](H_2O)_3$.

The crystal structure of *RbUAs* was refined in space group *P*4/*n* using the non-H atomic positions of Locock & Burns (2003a) for metazeunerite, $Cu[(UO_2)(AsO_4)]_2(H_2O)_8$, as a starting point. Because *RbUAs* was solved in a low-symmetry tetragonal space-group, the twin law $[010/100/00\bar{1}]$ was applied, and the structure was refined according to published methods (Jameson 1982, Herbst-Irmer & Sheldrick 1998), and resulted in a significant improvement of the agreement index ($R1$ = 1.9%). The twin-component scale factor refined to 14.6(2)%. The location of each H atom in these structures was not determined.

The crystal structures of *CsUP* and *CsHUAs* were solved by direct methods, and models in space group $P2_1/n$ converged. Because these compounds are respectively pseudo-tetragonal and pseudo-orthorhombic (Table 4) with β angles close to 90°, the twin law $[100/0\bar{1}0/00\bar{1}]$ was applied, and the structures were refined according to published methods (Jameson 1982, Herbst-Irmer & Sheldrick 1998), yielding agreement indices ($R1$) of 2.8% for *CsUP*, and 4.6% for *CsHUAs*, for the observed unique reflections ($|F_o| \geq 4\sigma_F$). The twin scale-factors refined to 0.26(5) and 3.0(2)% respectively, and are consistent with highly asymmetrical distributions of the twin components. The location of each H atom in these structures was not determined.

The atomic positional parameters are given in Table 5 for *LiUP*, Table 6 for *NaUP* and *NaUAs*, Table 7 for *KUAs*, Table 8 for *RbUP* and *RbUAs*,

TABLE 5. ATOMIC COORDINATES AND DISPLACEMENT PARAMETERS (Å^2) FOR *LiUP*, $Li[(UO_2)(PO_4)](H_2O)_4$

	x	*y*	*z*	U_{eq}
U(1)	¼	¼	0.0958(1)	0.013(1)
P(1)	¼	¾	0	0.014(1)
Li(1)	¼	¾	½	0.030(2)
O(1)	¼	¼	0.2889(3)	0.024(1)
O(2)	¼	¼	-0.0989(3)	0.024(1)
O(3)	0.5780(2)	0.2931(2)	0.0997(2)	0.021(1)
O(4)	0.1894(3)	-0.0373(3)	0.6309(2)	0.032(1)
H(1)	0.157(5)	-0.083(4)	0.731(2)	0.05[1]
H(2)	0.108(5)	0.076(4)	0.613(3)	0.05[1]

U_{eq} is defined as one third of the trace of the orthogonalized U_{ij} tensor.

[1] Value constrained during refinement.

TABLE 6. ATOMIC COORDINATES AND DISPLACEMENT PARAMETERS (Å^2) FOR *NaUP*, Na[$(UO_2)(PO_4)$]$(H_2O)_3$, AND *NaUAs*, Na[$(UO_2)(AsO_4)$]$(H_2O)_3$

NaUP	*x*	*y*	*z*	U_{eq}	*NaUAs*	*x*	*y*	*z*	U_{eq}
U(1)	¼	¼	0.0499(2)	0.017(1)	U(1)	¼	¼	0.0542(1)	0.018(1)
P(1)	¾	¼	0	0.021(1)	As(1)	¾	¼	0	0.020(1)
O(1)	¼	¼	0.1534(4)	0.032(1)	O(1)	¼	¼	0.1576(3)	0.031(1)
O(2)	¼	¼	0.9480(3)	0.032(1)	O(2)	¼	¼	0.9515(3)	0.036(1)
O(3)	0.7162(3)	0.0759(4)	0.4469(2)	0.028(1)	O(3)	0.7122(3)	0.0665(3)	0.4420(2)	0.029(1)
O(4)[1]	0.170(2)	0.9794(18)	0.3099(4)	0.188(4)	O(4)[1]	0.1625(17)	0.9864(16)	0.3068(3)	0.247(4)

U_{eq} is defined as one third of the trace of the orthogonalized U_{ij} tensor.
[1] O(4) fixed contents Na(1) 0.25, O 0.75, in accord with INAA results.

TABLE 7. ATOMIC COORDINATES AND DISPLACEMENT PARAMETERS (Å^2) FOR *KUAs*, K[$(UO_2)(AsO_4)$]$(H_2O)_3$

	x	*y*	*z*	U_{eq}
U(1)	¼	¼	0.0529(1)	0.014(1)
As(1)	¾	¼	0	0.016(1)
O(1)	¼	¼	0.1517(4)	0.027(1)
O(2)	¼	¼	0.9536(4)	0.030(2)
O(3)	0.7143(5)	0.0671(5)	0.4433(2)	0.020(1)
O(4)[1]	0.1624(7)	0.9909(6)	0.3135(3)	0.061(2)

U_{eq} is defined as one third of the trace of the orthogonalized U_{ij} tensor.
[1] O(4) refined contents: K(1) 0.227(15), O 0.773(15).

Table 9 for *AgUP* and *AgUAs*, Table 10 for *TlUP* and *TlUAs*, and Table 11 for *CsUP* and *CsHUAs*. Selected interatomic distances for *LiUP, NaUP, NaUAs, KUAs, RbUP, RbUAs, AgUP, AgUAs, TlUP*, and *TlUAs* are given in Table 12, and selected interatomic distances of *CsUP* and *CsHUAs* are listed in Table 13. Anisotropic displacement parameters, and observed and calculated structure-factors for these compounds are available from the Depository of Unpublished Data, CISTI, National Research Council, Ottawa, Ontario K1A 0S2, Canada. Bond-valence sums at the non-H cation sites for the twelve compounds are in Table 14, and were calculated using the parameters of Burns *et al.* (1997) for sixfold-coordinated U^{6+}, Brown & Altermatt (1985) for P^{5+}, As^{5+}, Li, Na, K, Rb, Ag and Cs, and R_0 = 1.927 Å, B = 0.50 Å for Tl (Locock & Burns 2003b). With the exception of Na and Ag, the bond-valence sums are in good agreement with expected formal valences.

Description of the Structures

LiUP is isostructural with its arsenate analogue, Li[$(UO_2)(AsO_4)$]$(H_2O)_4$ (Fitch *et al.* 1982a). It contains the well-known corrugated autunite-type sheet formed by the sharing of vertices between uranyl square bipyramids and phosphate tetrahedra (Fig. 2), with composition $[(UO_2)(PO_4)]^-$, which was originally described by Beintema (1938). The acute angle θ of the parallelogram formed between the tetrahedra and square bipyramids [parallel to (001), Fig. 2], defined as ∠O(3)–O(3)–O(3), is 75.3°. The interlayer Li(1) position is coordinated by four H_2O groups (Fig. 3), forming a tetragonal disphenoid, point group $\bar{4}$ (S_4 in Schoenflies

TABLE 8. ATOMIC COORDINATES AND DISPLACEMENT PARAMETERS (Å^2) FOR *RbUP*, Rb[$(UO_2)(PO_4)$]$(H_2O)_3$, AND *RbUAs*, Rb[$(UO_2)(AsO_4)$]$(H_2O)_3$

RbUP	*x*	*y*	*z*	U_{eq}	*RbUAs*	*x*	*y*	*z*	U_{eq}
U(1)	¼	¼	0.0481(1)	0.016(1)	U(1)	¼	¼	0.0543(1)	0.012(1)
P(1)	¾	¼	0	0.019(1)	U(2)	¼	¼	0.5513(1)	0.012(1)
O(1)	¼	¼	0.1468(3)	0.029(1)	As(1)	¼	¾	0	0.013(1)
O(2)	¼	¼	0.9487(3)	0.029(1)	As(2)	¼	¾	½	0.014(1)
O(3)	0.7270(4)	0.0756(4)	0.4492(2)	0.026(1)	O(1)	¼	¼	0.4504(4)	0.024(3)
O(4)[1]	0.1738(4)	0.9769(3)	0.3157(1)	0.055(1)	O(2)	¼	¼	-0.0449(4)	0.028(3)
					O(3)	¼	¼	0.6520(4)	0.022(2)
					O(4)	¼	¼	0.1560(4)	0.020(2)
					O(5)	0.2209(5)	0.9336(5)	0.0577(2)	0.020(1)
					O(6)	0.2236(6)	0.9353(6)	0.5567(2)	0.024(1)
					O(7)[2]	0.5217(2)	0.3446(2)	0.3003(1)	0.044(1)
					O(8)	0.1801(8)	0.5211(8)	-0.1910(3)	0.055(1)

U_{eq} is defined as one third of the trace of the orthogonalized U_{ij} tensor.
[1] O(4) refined contents: Rb(1) 0.187(4), O 0.813(4).
[2] O(7) refined contents: Rb(1) 0.500(2), O 0.500(2).

TABLE 9. ATOMIC COORDINATES AND DISPLACEMENT PARAMETERS (Å^2)
FOR *AgUP*, Ag[$(UO_2)(PO_4)$]$(H_2O)_3$, AND *AgUAs*, Ag[$(UO_2)(AsO_4)$]$(H_2O)_3$

AgUP	*x*	*y*	*z*	U_{eq}	*AgUAs*	*x*	*y*	*z*	U_{eq}
U(1)	¼	¼	0.0518(1)	0.013(1)	U(1)	¼	¼	0.0560(1)	0.014(1)
P(1)	¾	¼	0	0.016(1)	As(1)	¾	¼	0	0.016(1)
O(1)	¼	¼	0.1571(3)	0.025(1)	O(1)	¼	¼	0.1595(3)	0.025(1)
O(2)	¼	¼	0.9470(2)	0.026(1)	O(2)	¼	¼	0.9525(3)	0.027(1)
O(3)	0.7065(3)	0.0771(3)	0.4461(1)	0.023(1)	O(3)	0.6990(4)	0.0680(3)	0.4409(2)	0.023(1)
O(4)[1]	0.1626(2)	0.9991(2)	0.3161(1)	0.060(1)	O(4)[2]	0.1557(2)	0.0111(2)	0.3159(1)	0.064(1)

U_{eq} is defined as one third of the trace of the orthogonalized U_{ij} tensor.
[1] O(4) refined contents: Ag(1) 0.218(2), O 0.782(2).
[2] O(4) refined contents: Ag(1) 0.233(3), O 0.767(3).

TABLE 10. ATOMIC COORDINATES AND DISPLACEMENT PARAMETERS (Å^2)
FOR *TlUP*, Tl[$(UO_2)(PO_4)$]$(H_2O)_3$, AND *TlUAs*, Tl[$(UO_2)(AsO_4)$]$(H_2O)_3$

TlUP	*x*	*y*	*z*	U_{eq}	*TlUAs*	*x*	*y*	*z*	U_{eq}
U(1)	¼	¼	0.0483(1)	0.014(1)	U(1)	¼	¼	0.0529(1)	0.016(1)
P(1)	¾	¼	0	0.015(1)	As(1)	¾	¼	0	0.018(1)
O(1)	¼	¼	0.1490(6)	0.024(2)	O(1)	¼	¼	0.1512(5)	0.026(2)
O(2)	¼	¼	0.9483(5)	0.024(2)	O(2)	¼	¼	0.9548(5)	0.029(2)
O(3)	0.7279(4)	0.0740(4)	0.4491(2)	0.022(1)	O(3)	0.7191(4)	0.0659(5)	0.4437(2)	0.025(1)
O(4)[1]	0.1699(2)	0.9858(1)	0.3158(1)	0.054(1)	O(4)[2]	0.1707(2)	-0.0057(2)	0.3133(1)	0.063(1)

U_{eq} is defined as one third of the trace of the orthogonalized U_{ij} tensor.
[1] O(4) refined contents: Tl(1) 0.245(2), O 0.755(2).
[2] O(4) refined contents: Tl(1) 0.252(2), O 0.748(2).

TABLE 11. ATOMIC COORDINATES AND DISPLACEMENT PARAMETERS (Å^2)
FOR *CsUP*, $Cs_2[(UO_2)(PO_4)]_2(H_2O)_5$, AND *CsHUAs*, $Cs(H_3O)[(UO_2)(AsO_4)]_2(H_2O)_5$

CsUP	*x*	*y*	*z*	U_{eq}	*CsHUAs*	*x*	*y*	*z*	U_{eq}
U(1)	0.7443(1)	0.0002(1)	0.0470(1)	0.012(1)	U(1)	0.1252(1)	0.2461(1)	0.0531(1)	0.012(1)
U(2)	0.2551(1)	0.0035(1)	0.4497(1)	0.012(1)	U(2)	0.6245(1)	0.2443(1)	0.0540(1)	0.011(1)
P(1)	0.5002(2)	0.7457(2)	-0.0020(1)	0.014(1)	As(1)	0.3750(1)	0.2527(1)	0.0007(1)	0.013(1)
P(2)	0.0001(2)	0.7521(2)	-0.0028(1)	0.014(1)	As(2)	-0.1262(1)	0.2515(1)	-0.0015(1)	0.013(1)
Cs(1)	0.0894(1)	0.9071(1)	0.1944(1)	0.035(1)	Cs(1)	0.4521(1)	-0.6027(1)	0.2516(1)	0.046(1)
Cs(2)	0.8064(1)	0.3094(1)	0.2019(1)	0.041(1)	O(1)	0.6211(5)	0.2390(10)	-0.0479(4)	0.024(2)
O(1)	0.5832(4)	0.8391(4)	0.0492(3)	0.024(1)	O(2)	0.1229(5)	0.2450(10)	-0.0491(4)	0.021(2)
O(2)	0.4206(4)	0.1632(4)	0.4470(3)	0.019(1)	O(3)	0.6271(5)	0.2456(9)	0.1579(4)	0.017(2)
O(3)	0.0887(4)	0.1615(4)	0.4501(3)	0.022(1)	O(4)	0.1259(5)	0.2459(9)	0.1562(4)	0.019(2)
O(4)	0.0911(5)	0.8429(4)	0.4505(3)	0.027(1)	O(5)	0.3959(5)	0.0752(9)	-0.0605(4)	0.018(2)
O(5)	0.9113(4)	0.8448(4)	0.0448(3)	0.021(1)	O(6)	-0.1046(5)	0.0689(9)	-0.0594(4)	0.020(2)
O(6)	0.5873(4)	0.1696(4)	0.0567(3)	0.020(1)	O(7)	-0.0338(4)	0.2978(9)	0.0598(4)	0.016(2)
O(7)	0.4130(4)	0.8341(4)	0.4438(3)	0.020(1)	O(8)	0.4670(5)	0.2903(9)	0.0605(4)	0.019(2)
O(8)	0.7381(4)	0.0064(4)	-0.0526(2)	0.022(1)	O(9)	-0.2164(5)	0.2088(10)	0.0570(4)	0.018(2)
O(9)	0.2632(4)	0.0036(4)	0.5503(2)	0.023(1)	O(10)	0.2833(4)	0.2023(9)	0.0570(4)	0.019(2)
O(10)	0.2510(4)	0.0062(4)	0.3484(2)	0.020(1)	O(11)	0.3505(5)	0.4396(9)	-0.0555(4)	0.018(2)
O(11)	0.7520(4)	0.9959(4)	0.1485(2)	0.021(1)	O(12)	-0.1496(5)	0.4366(10)	-0.0584(4)	0.021(2)
O(12)	0.0960(4)	0.8350(4)	-0.0521(3)	0.021(1)	O(13)W	0.6636(6)	0.0071(12)	-0.1894(5)	0.040(2)
O(13)W	0.1653(5)	0.2024(5)	0.1907(3)	0.038(1)	O(14)W	0.1644(5)	-0.116(11)	-0.1934(4)	0.031(2)
O(14)W	0.4320(6)	0.1394(5)	0.1917(3)	0.047(2)	O(15)W	0.7386(6)	0.3735(15)	-0.1913(5)	0.054(3)
O(15)W	0.0759(6)	0.3580(5)	0.3070(3)	0.050(2)	O(16)W	0.0754(6)	0.5092(11)	-0.1881(5)	0.034(2)
O(16)W	0.9122(5)	0.0668(5)	0.3152(3)	0.040(1)	O(17)W	0.4892(5)	0.1658(11)	-0.1945(4)	0.030(2)
O(17)W	0.6127(6)	0.1265(5)	0.3120(3)	0.045(2)	O(18)M	0.2377(5)	0.3622(10)	-0.1865(4)	0.027(2)

U_{eq} is defined as one third of the trace of the orthogonalized U_{ij} tensor.
Suffix W indicates O atom of a water molecule, (H_2O); M indicates O atom of an oxonium group, $(H_3O)^+$.

notation). Hydrogen bonds link the interstitial H_2O group into square-planar sets, which are connected *via* the Li–O bonds (Fig. 4). Hydrogen bonds extend from these sets to the anions at the equatorial vertices of uranyl square bipyramids, which are also shared with phosphate tetrahedra (Fig. 3).

TABLE 12. SELECTED INTERATOMIC DISTANCES (Å)
FOR *LiUP, NaUP, NaUAs, KUAs, RbUP, RbUAs, AgUP, AgUAs, TlUP*, AND *TlUAs*

	LiUP			*NaUP*			*RbUP*			*AgUP*			*TlUP*	
U(1)-O(1)	1.765(3)		U(1)-O(1)	1.787(7)		U(1)-O(1)	1.774(6)		U(1)-O(1)	1.781(5)		U(1)-O(1)	1.799(9)	
U(1)-O(2)	1.779(3)		U(1)-O(2)	1.759(6)		U(1)-O(2)	1.788(6)		U(1)-O(2)	1.774(4)		U(1)-O(2)	1.810(11)	
U(1)-O(3)	2.3012(16)	x 4	U(1)-O(3)	2.282(3)	x 4	U(1)-O(3)	2.289(3)	x 4	U(1)-O(3)	2.288(2)	x 4	U(1)-O(3)	2.280(3)	x 4
<U(1)-O_{ap}>	1.77		<U(1)-O_{ap}>	1.77		<U(1)-O_{ap}>	1.78		<U(1)-O_{ap}>	1.78		<U(1)-O_{ap}>	1.80	
P(1)-O(3)	1.5335(15)	x 4	P(1)-O(3)	1.537(3)	x 4	P(1)-O(3)	1.535(3)	x 4	P(1)-O(3)	1.5360(19)	x 4	P(1)-O(3)	1.545(4)	x 4
Li(1)-O(4)	1.948(2)	x 4	Na(1)-O(4)	2.537(14)		Rb(1)-O(4)	2.795(4)		Ag(1)-O(4)	2.6050(16)	x 2	Tl(1)-O(4)	2.7408(16)	x 2
H(1)-O(4)	0.992(17)		Na(1)-O(4)	2.779(14)	x 2	Rb(1)-O(4)	2.811(3)	x 2	Ag(1)-O(3)	2.689(2)		Tl(1)-O(4)	2.825(3)	
H(2)-O(4)	0.983(18)		Na(1)-O(3)	2.807(8)		Rb(1)-O(3)	2.877(4)		Ag(1)-O(4)	2.743(2)		Tl(1)-O(3)	2.907(4)	
			Na(1)-O(2)	3.090(10)		Rb(1)-O(2)	3.110(5)		Ag(1)-O(2)	2.883(3)		Tl(1)-O(2)	3.072(7)	
	RbUAs		Na(1)-O(1)	3.341(9)		Rb(1)-O(4)	3.357(4)		Ag(1)-O(1)	3.262(4)		Tl(1)-O(1)	3.439(3)	
U(1)-O(2)	1.750(8)		Na(1)-O(4)	3.38(3)		Rb(1)-O(1)	3.437(3)		Ag(1)-O(1)	3.3726(14)		Tl(1)-O(4)	3.495(2)	
U(1)-O(4)	1.795(8)		<Na(1)-O>	2.96		<Rb(1)-O>	3.03		<Ag(1)-O>	2.88		<Tl(1)-O>	3.03	
U(1)-O(5)	2.285(4)	x 4												
<U(1)-O_{ap}>	1.77													
U(2)-O(3)	1.776(8)													
U(2)-O(1)	1.780(6)			*NaUAs*			*KUAs*			*AgUAs*			*TlUAs*	
U(2)-O(6)	2.273(4)	x 4	U(1)-O(1)	1.791(5)		U(1)-O(1)	1.766(8)		U(1)-O(1)	1.765(6)		U(1)-O(1)	1.766(9)	
<U(2)-O_{ap}>	1.78		U(1)-O(2)	1.779(5)		U(1)-O(2)	1.773(8)		U(1)-O(2)	1.765(5)		U(1)-O(2)	1.764(8)	
			U(1)-O(3)	2.280(2)	x 4	U(1)-O(3)	2.288(4)	x 4	U(1)-O(3)	2.284(2)		U(1)-O(3)	2.283(3)	x 4
As(1)-O(5)	1.680(4)	x 4	<U(1)-O_{ap}>	1.79		<U(1)-O_{ap}>	1.77		<U(1)-O_{ap}>	1.77		<U(1)-O_{ap}>	1.77	
As(2)-O(6)	1.677(4)	x 4	As(1)-O(3)	1.675(2)	x 4	As(1)-O(3)	1.676(4)	x 4	As(1)-O(3)	1.676(2)		As(1)-O(3)	1.681(3)	x 4
Rb(1)-O(7)	2.9258(16)	x 2	Na(1)-O(4)	2.479(15)		K(1)-O(4)	2.749(9)		Ag(1)-O(4)	2.576(2)	x 2	Tl(1)-O(4)	2.7219(16)	x 2
Rb(1)-O(6)	2.983(4)		Na(1)-O(4)	2.808(13)	x 2	K(1)-O(4)	2.772(6)	x 2	Ag(1)-O(3)	2.673(3)		Tl(1)-O(4)	2.827(2)	
Rb(1)-O(8)	3.042(6)		Na(1)-O(3)	2.824(7)		K(1)-O(3)	2.831(6)		Ag(1)-O(4)	2.801(3)		Tl(1)-O(3)	2.901(4)	
Rb(1)-O(8)	3.104(5)		Na(1)-O(2)	3.198(9)		K(1)-O(2)	3.180(7)		Ag(1)-O(2)	2.955(4)		Tl(1)-O(2)	3.188(7)	
Rb(1)-O(8)	3.229(5)		Na(1)-O(1)	3.260(8)		K(1)-O(1)	3.479(5)		Ag(1)-O(1)	3.4460(18)		Tl(1)-O(1)	3.556(2)	
Rb(1)-O(4)	3.280(6)		Na(1)-O(1)	3.455(9)		K(1)-O(1)	3.492(8)		Ag(1)-O(4)	3.642(3)		Tl(1)-O(3)	3.605(4)	
<Rb(1)-O>	3.07		<Na(1)-O>	2.98		<K(1)-O>	3.04		<Ag(1)-O>	2.95		<Tl(1)-O>	3.07	

Note: Interlayer cations limited to 7-fold coordination, with the exception of Li.

The compounds *NaUP, NaUAs, KUAs, RbUP, AgUP, AgUAs, TlUP*, and *TlUAs* are all isostructural in space group *P4/ncc*, as are the K, NH_4^+ and H_3O^+ compounds listed in Table 1. In this structure type (Fig. 5), first described by Ross & Evans (1964), the autunite-type sheet consists of uranyl square bipyramids and either phosphate or arsenate tetrahedra, and the acute angles {$\theta = \angle O(3)–O(3)–O(3)$} of the parallelograms formed between the tetrahedra and square bipyramids change slightly because of the rotation of the polyhedra (the axis of rotation is normal to the plane of the sheet, along [001]), and depend on the nature of the interlayer cation and the type of tetrahedron present: *NaUP* 78.4°, *NaUAs* 77.4°, *KUAs* 78.2°, *RbUP* 82.0°, *AgUP* 75.2°, *AgUAs* 73.3°, *TlUP* 82.3°, and *TlUAs* 79.7°. The interlayer cations and oxygen are disordered on the single symmetrically independent interlayer position, O(4), and for reasons of charge balance, have a maximum occupancy of 25% of this site. Although the H positions were not located in the structures presented here, possible H-bonds can be suggested on the basis of O...O distances (Fig. 6) that correspond to the four shortest interlayer distances for each structure listed in Table 12. Hydrogen bonds (and cation–oxygen bonds from 25% or less of the sites, depending on cation occupancy) link the interstitial H_2O group into square-planar sets, and similarly connect the square planar sets together, and extend to the anions at the equatorial vertices of uranyl square bipyramids that are also shared with tetrahedra (Fig. 5).

The displacement parameters of the interlayer positions in *NaUP* and *NaUAs* (Table 6) are significantly larger than expected for well-behaved atoms in well-refined structures. Difference-Fourier maps plotted along [100] (Figs. 7a, b) and along [001] (Figs. 8a, b) reveal only a single center of electron density associated with this position. The site was assigned ideal occupancy (Na 0.25, O 0.75) in accord with the INAA results. In the nomenclature of chemical hardness (Pearson 1993), Na is a hard Lewis acid, whose elec-

TABLE 13. SELECTED INTERATOMIC DISTANCES (Å) FOR *CsUP* AND *CsHUAs*

U(1)-O(8)	1.760(4)	Cs(1)-O(13)W	3.035(5)	U(1)-O(2)	1.760(7)	Cs(1)-O(4)	3.167(7)
U(1)-O(11)	1.792(4)	Cs(1)-O(8)	3.157(4)	U(1)-O(4)	1.775(7)	Cs(1)-O(3)	3.188(6)
U(1)-O(1)	2.258(4)	Cs(1)-O(16)W	3.191(5)	U(1)-O(6)	2.272(7)	Cs(1)-O(14)W	3.260(8)
U(1)-O(5)	2.261(4)	Cs(1)-O(5)	3.222(5)	U(1)-O(10)	2.277(6)	Cs(1)-O(15)W	3.323(10)
U(1)-O(12)	2.277(4)	Cs(1)-O(10)	3.292(4)	U(1)-O(12)	2.295(7)	Cs(1)-O(6)	3.378(7)
U(1)-O(6)	2.298(4)	Cs(1)-O(15)W	3.341(6)	U(1)-O(7)	2.302(6)	Cs(1)-O(17)W	3.382(8)
<U(1)-O_{ap}>	1.78	Cs(1)-O(14)W	3.345(5)	<U(1)-O_{ap}>	1.77	Cs(1)-O(8)	3.390(7)
<U(1)-O_{eq}>	2.27	Cs(1)-O(17)W	3.434(5)	<U(1)-O_{eq}>	2.29	Cs(1)-O(13)W	3.485(9)
		Cs(1)-O(2)	3.483(4)			Cs(1)-O(16)W	3.540(8)
U(2)-O(9)	1.777(4)	<Cs(1)-O>	3.28	U(2)-O(1)	1.756(7)	<Cs(1)-O>	3.35
U(2)-O(10)	1.788(4)			U(2)-O(3)	1.789(7)		
U(2)-O(3)	2.274(4)	Cs(2)-O(12)	3.164(5)	U(2)-O(8)	2.275(7)	O(18)M-O(16)W	2.54(1)
U(2)-O(4)	2.276(4)	Cs(2)-O(17)W	3.266(5)	U(2)-O(9)	2.283(7)	O(18)M-O(14)W	2.67(1)
U(2)-O(2)	2.280(4)	Cs(2)-O(15)W	3.269(6)	U(2)-O(11)	2.286(6)	O(18)M-O(11)	2.80(1)
U(2)-O(7)	2.300(4)	Cs(2)-O(11)	3.283(4)	U(2)-O(5)	2.303(7)	O(18)M-O(14)W	2.87(1)
<U(2)-O_{ap}>	1.78	Cs(2)-O(9)	3.285(4)	<U(2)-O_{ap}>	1.77		
<U(2)-O_{eq}>	2.28	Cs(2)-O(17)W	3.286(6)	<U(2)-O_{eq}>	2.29		
		Cs(2)-O(16)W	3.301(5)				
P(1)-O(4)	1.515(5)	Cs(2)-O(11)	3.303(4)	As(1)-O(8)	1.674(7)		
P(1)-O(3)	1.524(5)	Cs(2)-O(16)W	3.362(5)	As(1)-O(5)	1.679(7)		
P(1)-O(1)	1.531(5)	<Cs(2)-O>	3.28	As(1)-O(11)	1.681(6)		
P(1)-O(6)	1.542(5)			As(1)-O(10)	1.682(7)		
<P(1)-O>	1.53			<As(1)-O>	1.68		
P(2)-O(5)	1.529(4)			As(2)-O(6)	1.674(7)		
P(2)-O(12)	1.532(4)			As(2)-O(12)	1.675(7)		
P(2)-O(7)	1.533(4)			As(2)-O(9)	1.677(7)		
P(2)-O(2)	1.535(5)			As(2)-O(7)	1.705(7)		
<P(2)-O>	1.53			<As(2)-O>	1.68		

Cs positions limited to 9-fold coordination. Suffix W indicates O atom of a water molecule, (H_2O); M indicates O atom of an oxonium group, $(H_3O)^+$.

tronic configuration tends toward spherical symmetry and is not easily polarized (deformed). The bond distances to Na in *NaUP* and *NaUAs* (Table 12) are mostly considerably larger than would be predicted for normal [7]Na–O bonds, ~2.5 Å, on the basis of ionic radii (Shannon 1976). However, the four shortest distances in each case are reasonable separation distances for oxygen atoms involved in hydrogen bonding (Jeffrey 1997). The Na atoms substituted for O at the interlayer O(4) position in *NaUP* and *NaUAs* may be analogous to Na in albite, and involve either a time average of highly anisotropic thermal vibration, or a space average of multiple (currently unresolved) Na positions (Alberti *et al.* 2003). In this regard, it is notable that the ionic conductivity of *NaUP* is two orders of magnitude higher than the conductivities of its K, Ag or NH_4^+ isostructures (Johnson *et al.* 1981, Pham-Thi & Colomban 1985). The irregular behavior of Na in *NaUP* and *NaUAs* may help to explain the low bond-valence sums for Na in these structures (Table 14).

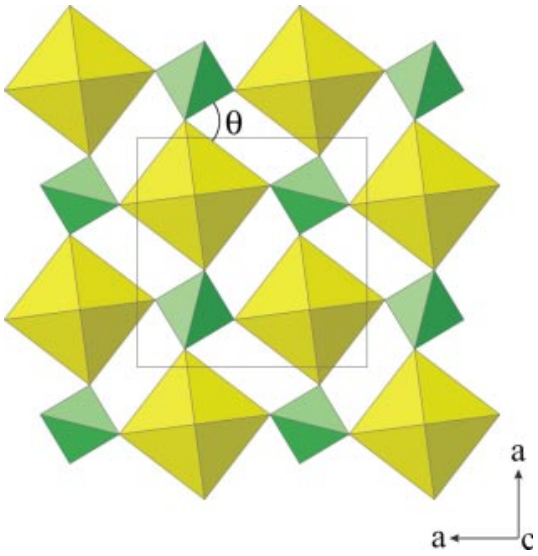

FIG. 2. The autunite-type sheet found in *LiUP*, $Li[(UO_2)(PO_4)](H_2O)_4$, formed by the sharing of vertices between uranyl square bipyramids and phosphate tetrahedra. The acute angle θ of the parallelogram formed between the tetrahedra and square bipyramids is equal to 75.3°.

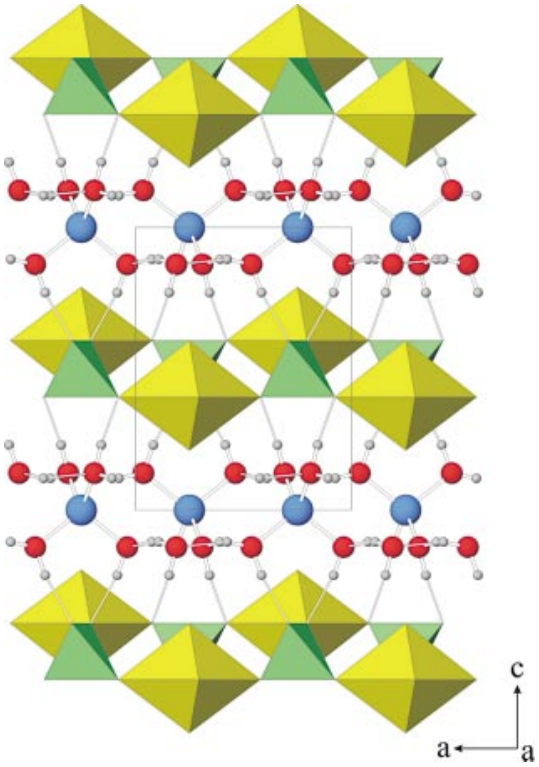

FIG. 3. The structure of *LiUP*, $Li[(UO_2)(PO_4)](H_2O)_4$, projected along [100]. Uranyl polyhedra are yellow, phosphate tetrahedra are green, lithium atoms are blue, O atoms of H_2O groups are shown as red spheres, hydrogen atoms are shown as gray spheres, O–H bonds as thick rods, and H...O bonds as thin rods.

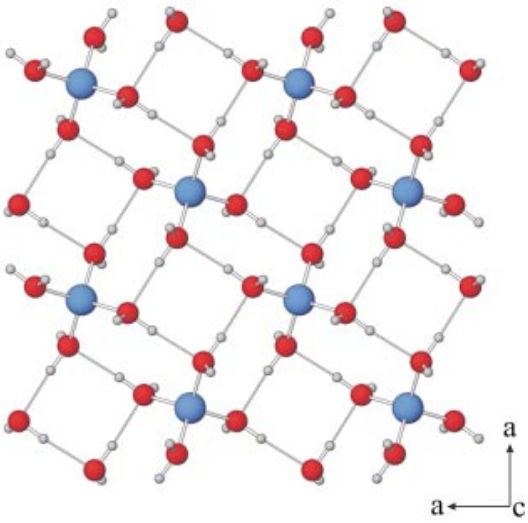

FIG. 4. The interlayer contents of *LiUP*, $Li[(UO_2)(PO_4)](H_2O)_4$, projected along [001]. Lithium atoms are blue, O atoms of H_2O groups are shown as red spheres, hydrogen atoms are shown as gray spheres, O–H bonds as thick rods, and H...O bonds as thin rods.

Although on average Ag is only 8% larger than Na for the same coordination number (Shannon 1976), it does not exhibit similarly anomalous behavior in this structure type. The displacement parameters of the interlayer positions in *AgUP* and *AgUAs* (Table 9) are reasonable, even though the interatomic distances (Table 12) are mostly longer than would be predicted for normal [7]Ag–O bonds, ~2.6 Å, on the basis of ionic radii (Shannon 1976). The long interatomic distances lead to low bond-valence sums for Ag (Table 14) using conventional bond-valence parameters (Brown & Altermatt 1985). A similarly low bond-valence sum for Ag has been noted in the structure of argentojarosite, for which the mean Ag–O distance is 2.84 Å for formal 12-fold coordination (Groat *et al.* 2003). Silver is a relatively soft Lewis acid (Pearson 1993), whose electronic configuration is relatively easily polarized. The soft acid – hard base Ag–O interactions may not be well modeled with conventional bond-valence parameters; for polarizable cations, it has been suggested that values of the B bond-valence parameter larger than 0.37 Å are appropriate (Krivovichev & Brown 2001, Adams 2001).

RbUAs is not isostructural with its phosphate analogue, *RbUP*, having been solved and refined in space group *P*4/*n* rather than *P*4/*ncc*. *RbUAs* has two U positions and two As positions, with two symmetrically independent autunite-type sheets (Fig. 9). The acute angles of the parallelograms formed between the tetrahedra and square bipyramids in the two sheets are: θ = 80.4° <O(4)–O(4)–O(4), and θ = 81.2° <O(5)–O(5)–O(5). The interlayer contains two symmetrically independent sites, one of which, O(8), comprises a H_2O group, whereas the O(7) position contains Rb disordered with the oxygen of a H_2O group. For reasons of charge balance, Rb has a maximum occupancy of 50% of this site; the O(7) site occupancy was refined (Table 8) and yields the following empirical formula: $Rb[(UO_2)(AsO_4)](H_2O)_3$. Although the H positions were not located in this structure, possible H-bonds can be suggested based on O...O distances of ~3 Å (Fig. 10). Hydrogen bonds [and cation–oxygen bonds from 50% of the O(7) sites, depending on local occupancy] link the interstitial H_2O groups into square-planar sets, and similarly connect the square planar sets together, and extend to the anions at the equatorial vertices of uranyl square bipyramids that are also shared with tetrahedra (Fig. 9). The presence of Rb in the O(7) site leads to further bonds (randomly distributed over half of the sites

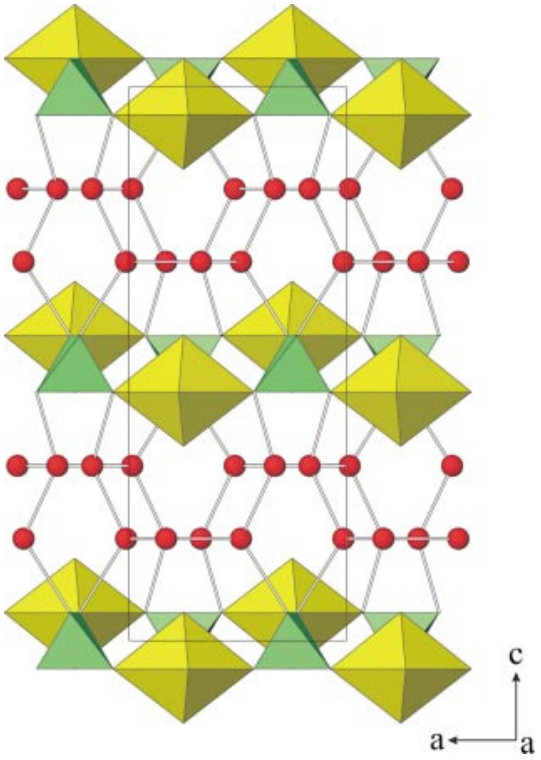

FIG. 5. The structure of monovalent meta-autunite compounds with space group *P*4/*ncc*, projected along [100]. Uranyl polyhedra are yellow, and the tetrahedra are green. The monovalent cations and H_2O groups are disordered on the interlayer site (shown in red), with maximum occupancy of 25% of the site. The O...O distances, consistent with hydrogen bonds (and cation–oxygen bonds), are shown.

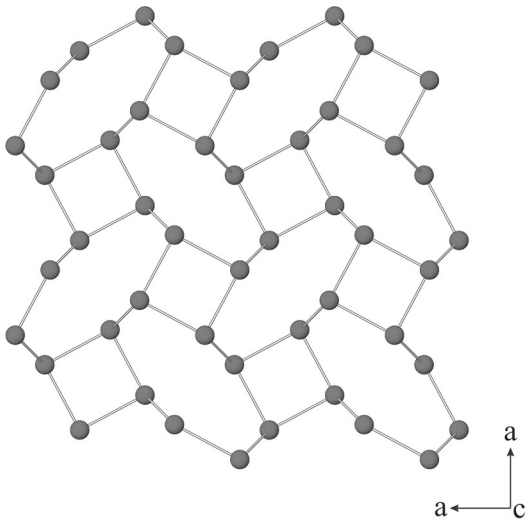

FIG. 6. The interlayer of monovalent meta-autunite compounds with space group *P*4/*ncc*, projected along [001]. The O...O distances, consistent with hydrogen bonds (and cation–oxygen bonds), are shown.

in accord with the Rb occupancy) connecting the sets such that each square set is 3-connected to each neighboring square set (Fig. 10), rather than 1-connected as in the *P*4/*ncc* structures (Fig. 6). Even longer interatomic distances (Table 12) from Rb to the uranyl ion oxygen atoms may serve to link the sheets on either side directly through the O(7) position. The structure of *RbUAs* is closely related to that of metazeunerite; the two uranyl arsenates are isostructural, with the exception of the differing positions of Rb and Cu and their interlayer H_2O groups. The position equivalent to the Cu site in metazeunerite is empty in *RbUAs*, and the O(7) position in *RbUAs*, which contains both Rb and O, corresponds to the OW(7) site in metazeunerite, in which it is fully occupied by oxygen (Locock & Burns 2003a). The structural similarity of *RbUAs* and metazeunerite may indicate a possible mechanism of solid solution between (some) members of the meta-autunite group with monovalent interlayer cations, and those with divalent interlayer cations. In the case of the Cu^{2+}–Rb^{+} uranyl arsenate system, the substitution can be written as follows: $Cu_{0.5x}\,Rb_{2-x}\,[(UO_2)(AsO_4)]_2\,(H_2O)_{6+x}$, where $0 \le x \le 2$.

CsUP contains the autunite-type sheet, with Cs atoms and H_2O groups located in the interlayer between the sheets (Fig. 11), but the orientation of its cell and its symmetry differ from the tetragonal meta-autunite structures. The mean *a* cell dimension of the tetragonal uranyl phosphate members of the meta-autunite group is about 7.0 Å, whereas the *a* and *b* unit-cell dimensions of pseudo-tetragonal *CsUP* average 9.91 Å, very close to the product of $\sqrt{2} * 7$ Å. The acute angle, θ, of the quadrilaterals formed between the phosphate tetrahedra and uranyl square bipyramids in *CsUP* range from 85.5 to 89.0°, a difference averaging about 10% from the structures described previously herein. The polyhedra in the autunite-type sheet of *CsUP* therefore form a nearly rectilinear pattern (Fig. 12). Because the autunite-type sheet is made up of vertex-sharing polyhedra, it has a significant degree of structural flexibility and can vary its geometry to accommodate different interlayer contents. There are two symmetrically distinct Cs positions, each of which is coordinated by five H_2O groups in the

TABLE 14. BOND VALENCE SUMS FOR THE CATIONS

LiUP	sum (*vu*)	*NaUP*	sum (*vu*)	*NaUAs*	sum (*vu*)
U(1)	6.11	U(1)	6.19	U(1)	6.13
P(1)	5.01	P(1)	4.97	As(1)	5.13
Li(1)	1.09	Na(1)	0.41	Na(1)	0.41
AgUP		*AgUAs*		*KUAs*	
U(1)	6.14	U(1)	6.23	U(1)	6.19
P(1)	4.98	As(1)	5.12	As(1)	5.12
Ag(1)	0.54	Ag(1)	0.53	K(1)	0.81
TlUP		*TlUAs*		*RbUP*	
U(1)	6.01	U(1)	6.24	U(1)	6.11
P(1)	4.86	As(1)	5.05	P(1)	4.99
Tl(1)	0.89	Tl(1)	0.87	Rb(1)	1.08
RbUAs		*CsUP*		*CsHUAs*	
U(1)	6.18	U(1)	6.22	U(1)	6.21
U(2)	6.20	U(2)	6.13	U(2)	6.17
As(1)	5.06	P(1)	5.09	As(1)	5.07
As(2)	5.10	P(2)	5.03	As(2)	5.03
Rb(1)	0.84	Cs(1)	0.94	Cs(1)	0.77
		Cs(2)	0.88		

Bond-valence sums were calculated assuming full occupancies of atomic sites.

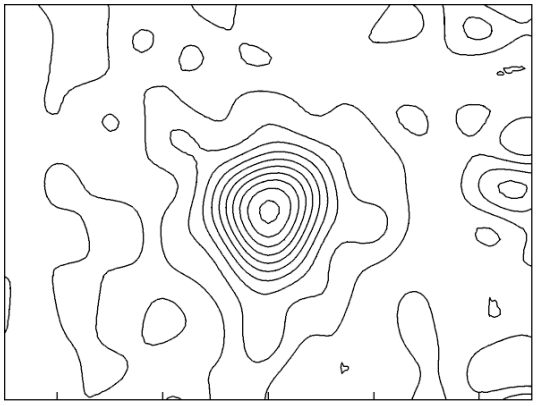

a)

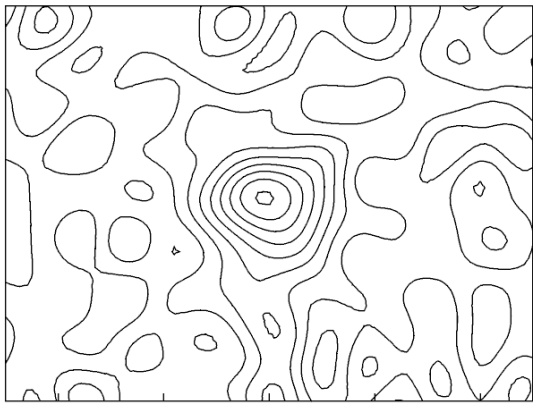

b)

FIG. 7. (a) Difference-Fourier map of the O(4) position in *NaUP*, $Na[(UO_2)(PO_4)](H_2O)_3$, projected along [100]. (b) Difference-Fourier map of the O(4) position in *NaUAs*, $Na[(UO_2)(AsO_4)](H_2O)_3$, projected along [100]. The X-axis scale is in ångströms, and the contours start at 0.5 *e* $Å^{-3}$, with a contour interval of 0.5 *e* $Å^{-3}$.

interlayer and four oxygen atoms of the uranyl phosphate sheet (Table 13). The sharing of two H_2O groups between the Cs(2) sites forms undulating chains along [010]; these chains are connected through Cs(1) positions and H_2O groups (Fig. 13). The bonds from Cs to oxygen atoms of the uranyl square bipyramids also serve to link the sheets directly (Fig. 11).

In contrast to *CsUP*, the autunite-type sheet found in *CsHUAs* is geometrically similar to those of the tetragonal meta-autunite structures; the acute angle, θ, of the quadrilaterals formed between the arsenate tetrahedra and uranyl square bipyramids in *CsHUAs* range from 74.0 to 77.2°. The interlayer of *CsHUAs* contains one Cs position coordinated by five H_2O groups in the interlayer and four oxygen atoms of the uranyl arsenate sheet (Table 13), and a further interlayer oxygen atom that does not coordinate Cs (Fig. 14). For reasons of charge balance, this oxygen atom, O(18)M, is assigned as an oxonium group, H_3O^+ (Leigh 1990), yielding the chemical formula $Cs(H_3O)[(UO_2)(AsO_4)]_2(H_2O)_5$. The unit cell of *CsHUAs* is pseudo-orthorhombic (Table 4), with an *a* cell dimension double that of the tetragonal meta-autunite uranyl arsenate structures. The doubling of the unit cell is an expression of the non-equivalence of the distinct H_3O^+ group and the Cs position in the interlayer. The oxonium group serves to link the H_2O-coordinated Cs ions into double chains along [010] (Fig. 15). The uranyl arsenate sheets are linked by hydrogen bonding and directly by the bonds from Cs to oxygen atoms of the uranyl square bipyramids (Fig. 14).

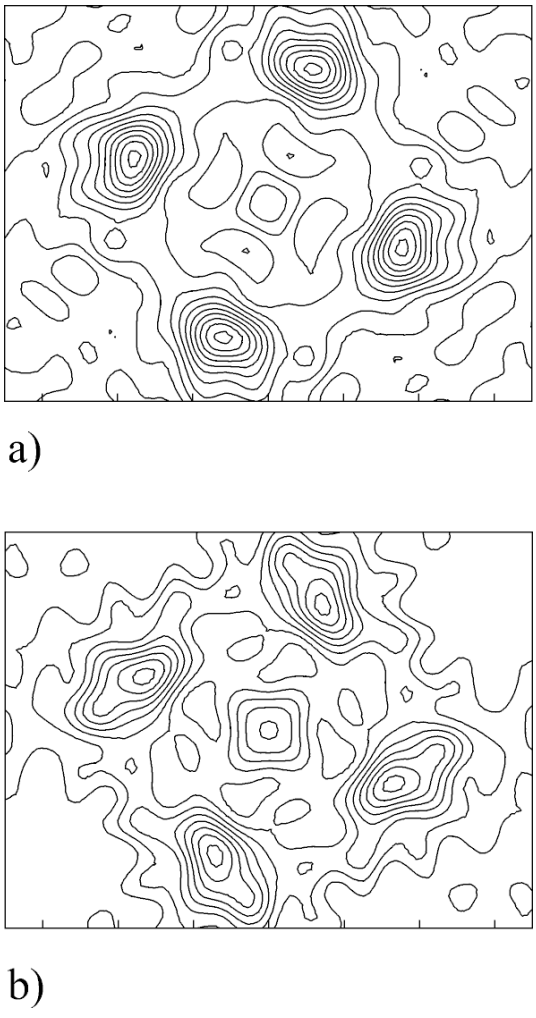

FIG. 8. (a) Difference-Fourier map showing the fourfold symmetry of the O(4) position in *NaUP*, $Na[(UO_2)(PO_4)](H_2O)_3$, projected along [001]. (b) Difference-Fourier map showing the fourfold symmetry of the O(4) position in *NaUAs*, $Na[(UO_2)(AsO_4)](H_2O)_3$, projected along [001]. The X-axis scale is in ångströms, and the contours start at 0.5 *e* $Å^{-3}$, with a contour interval of 0.5 *e* $Å^{-3}$.

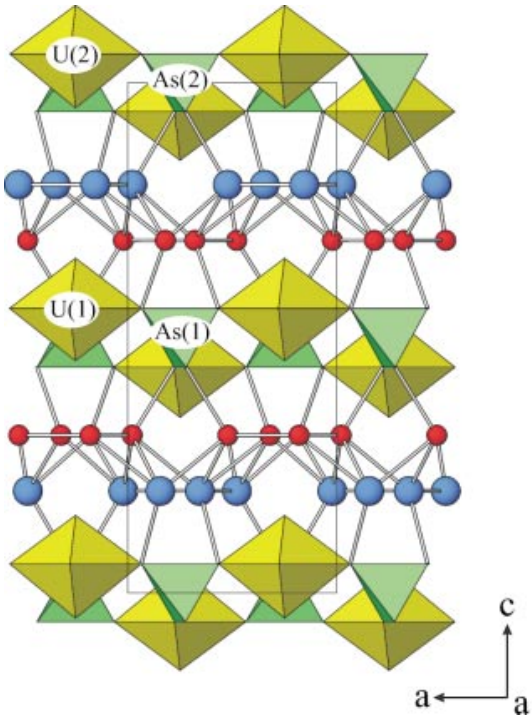

FIG. 9. The structure of *RbUAs*, $Rb[(UO_2)(AsO_4)](H_2O)_3$, projected along [100]. Uranyl polyhedra are yellow, and phosphate tetrahedra are green. The O(7) site is shown in blue and has a refined occupancy of Rb 50%, O 50%. The O(8) site is shown in red. The oxygen atoms of the interlayer sites correspond to H_2O groups. For clarity, interatomic distances longer than 3.25 Å are not shown.

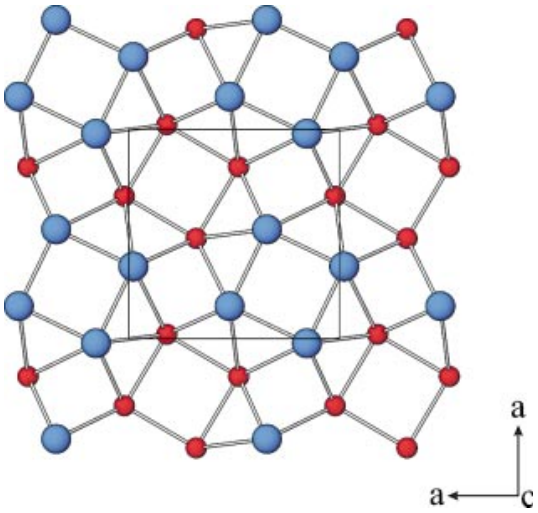

FIG. 10. The interlayer contents of *RbUAs*, Rb[$(UO_2)(AsO_4)$]$(H_2O)_3$, projected along [001]. The O(7) site is shown in blue and has an occupancy of Rb 50%, O 50%. The O(8) site is shown in red. The oxygen atoms of the interlayer sites correspond to H_2O groups. For clarity, interatomic distances longer than 3.25 Å are not shown.

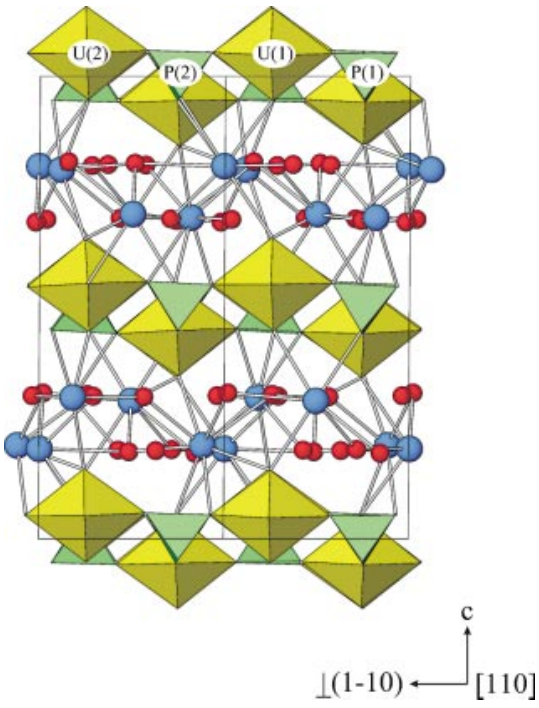

FIG. 11. The structure of *CsUP*, $Cs_2[(UO_2)(PO_4)]_2(H_2O)_5$, projected along [110]. Uranyl polyhedra are yellow, phosphate tetrahedra are green, cesium atoms are blue, and H_2O groups are shown as red spheres.

DISCUSSION

Interstitial low-valence cations are generally considered to play relatively passive charge-balancing and space-filling roles in inorganic structures, and to exert only subtle influences upon the crystallization of extended inorganic structures (Bean & Albrecht-Schmitt 2001, Hawthorne 1997). In compounds of the meta-autunite group with solely monovalent interlayer cations, the symmetries and hydration states observed are a function of the size of these cations.

Lithium is the smallest cation, with effective ionic radius: $^{[4]}Li^+$ 0.59 Å (Shannon 1976) and occurs at an interstitial site in between the squares of hydrogen-bonded H_2O molecules (Fig. 4), yielding the stoichiometry $Li[(UO_2)(XO_4)](H_2O)_4$. The compounds *LiUP* and its arsenate analogue adopt the low-symmetry tetragonal space-group *P*4/*n*.

Despite a wide range in effective ionic radius [$^{[7]}Na^+$ 1.12 Å, $^{[7]}Ag^+$ 1.22 Å, $^{[7]}K^+$ 1.46 Å, $^{[7]}Tl^+$ 1.54 Å (Shannon 1976, Tl value interpolated)], meta-autunite-group compounds with these cations are isostructural and adopt the same high-symmetry tetragonal structure (space group *P*4/*ncc*) as the ammonium and oxonium members. Although the *c* cell dimension of these compounds is almost double those of the analogous Li compounds (Tables 1, 4), their interlayer spacings are smaller (*e.g.*, in the uranyl phosphates: *LiUP* = 9.14 Å, *AgUP* = 8.47 Å and uramphite = 9.05 Å). This disparity may be attributed to the different method of incorporation of the interstitial cations, which randomly substitute for H_2O groups in the interlayer of the *P*4/*ncc* structures, yielding the stoichiometry $M[(UO_2)(XO_4)]$

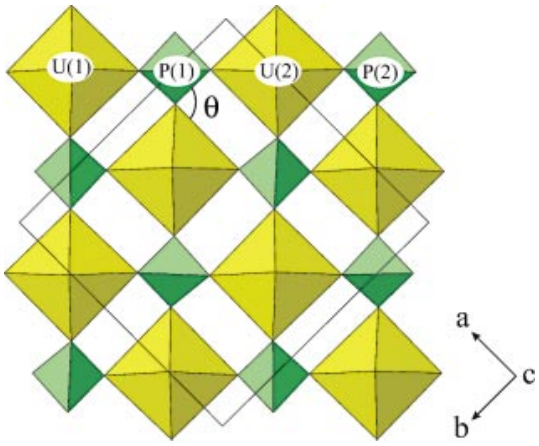

FIG. 12. The autunite-type sheet found in *CsUP*, $Cs_2[(UO_2)(PO_4)]_2(H_2O)_5$, projected along [001]. The acute angle θ of the quadrilateral formed between the tetrahedra and square bipyramids ranges from 85.5 to 89.0°; the polyhedra form a nearly rectilinear pattern.

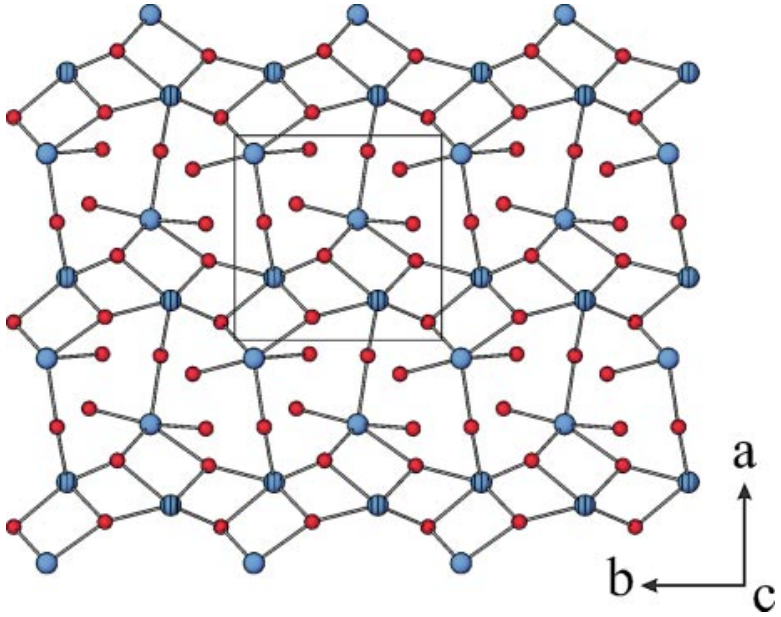

FIG. 13. The interlayer contents of *CsUP*, $Cs_2[(UO_2)(PO_4)]_2(H_2O)_5$, projected along [001]. The Cs(1) site is shown in solid blue, the Cs(2) site as striped blue spheres, and the H_2O groups are shown as red spheres.

$(H_2O)_3$. This formula can be rewritten as $\{M(H_2O)_3\}[(UO_2)(XO_4)]$, to emphasize the substitutional relationship of the interlayer cations and H_2O groups. The position corresponding to the Li site is empty in this structure type, and the squares of H_2O molecules are connected directly by hydrogen bonds (Fig. 6); thus, the separation between the H_2O squares is decreased and the interlayer spacings are smaller.

In general, phosphates are isostructural with their chemically corresponding arsenates, but this is not true of the Rb members (effective ionic radius $^{[7]}Rb^+$ 1.56 Å, Shannon 1976) of the meta-autunite group; *RbUP* adopts the *P4/ncc* structure type, whereas its chemical analogue *RbUAs* crystallizes in *P4/n*, with the identical hydration state. The *c* cell dimension of *RbUAs* (17.64 Å) is smaller than that of *RbUP* (17.98 Å) despite the presence of the larger As cation: $^{[4]}As^{5+}$ 0.335 Å, $^{[4]}P^{5+}$ 0.17 Å (Shannon 1976). Similar differences of 0.3 to 0.5 Å in the *c* dimensions of these compounds have been reported previously on the basis of powder X-ray-diffraction data (Schulte 1965, Chernorukov *et al.* 1994a, b). The smaller *c* cell dimension and lower symmetry of *RbUAs* are consistent with its different method of incorporation of Rb, which in *RbUAs* substitutes randomly for H_2O on only one of the two symmetrically independent interlayer positions (Fig. 9). The lack of isotypism in the Rb members of the meta-autunite group is unexpected, especially as the Li, Na, K, Ag, Tl, oxonium, and ammonium uranyl phosphates are all isostructural with their chemically corresponding uranyl arsenates. In *RbUAs*, there appears to be a cooperative effect between As and Rb in the formation of the structure, presumably to maintain mean Rb–O interatomic distances at reasonable values (~3.0–3.1 Å). This effect has been observed previously in the homeotypic framework structures of $Rb_2(UO_2)[(UO_2)(PO_4)]_4(H_2O)_2$, space group *Cm*, and $Rb_2(UO_2)[(UO_2)(AsO_4)]_4(H_2O)_{4.5}$, space group *C2/m* (Locock & Burns 2002, 2003c).

The Cs members of the meta-autunite group adopt monoclinic symmetry, and hydration states that differ from the tetragonal members of the group (Schulte 1965, Marković *et al.* 1988, Chernorukov *et al.* 1994a, b). These differences result from the differing configurations of the interlayer of the Cs compounds (Figs. 13, 15), which in turn are a function of the large size of the Cs cation: $^{[9]}Cs^+$ 1.78 Å (Shannon 1976). Whereas the meta-autunite structures with moderate-size monovalent cations (Na^+, K^+, Rb^+, Ag^+, Tl^+, and NH_4^+) can form isotypic solid-solution series with H_3O^+ (Schulte 1965, Ross & Evans 1965, Walenta 1965, Chernorukov *et al.* 2002), in *CsHUAs*, Cs and H_3O^+ adopt independent crystallographic sites (Fig. 14). The size difference between Cs and the other monovalent cations probably prevents their direct substitution, and may limit the extent of solid solution.

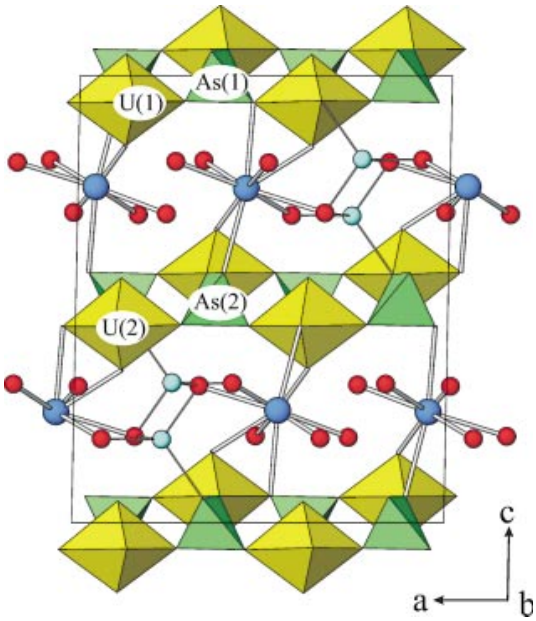

FIG. 14. The structure of *CsHUAs*, $Cs(H_3O)[(UO_2)(AsO_4)]_2(H_2O)_5$, projected along [010]. Uranyl polyhedra are yellow, phosphate tetrahedra are green, cesium atoms are dark blue large spheres, oxonium groups are pale blue small spheres, and H_2O groups are shown as red spheres. For clarity, only Cs–O bonds and $H_2O...H_3O^+$ interatomic distances are shown.

Higher hydration states of Na compounds

The sodium compounds characterized in this work, *NaUP* and *NaUAs*, have the stoichiometry $Na[(UO_2)(XO_4)](H_2O)_3$, *c* cell dimensions of ~17.2–17.3 Å (Table 4), and correspond to the mineral species sodium meta-autunite and the unfortunately named sodium uranospinite, respectively (Gaines *et al.* 1997, Anthony *et al.* 2000). However, higher hydrates have been noted in natural and synthetic samples. Chernikov & Organova (1996) described a natural specimen of sodium uranyl phosphate hydrate with *c'* = 8.99 Å (corresponding to a *c* cell dimension of 17.98 Å), stoichiometry $Na[(UO_2)(PO_4)](H_2O)_{5–6}$, and referred to this as "natroautunite" (sodium autunite), although this is not an approved name of a mineral species (Puziewicz 1995). Walenta (1965) discussed a synthetic sodium uranyl arsenate hydrate with a *c* cell dimension of 21.92 Å, stoichiometry $Na[(UO_2)(AsO_4)](H_2O)_5$, and referred to this as "Natrium-uranospinit" (sodium uranospinite), giving the name "Meta-Natrium-uranospinit" (sodium meta-uranospinite) to the lower hydrate $Na[(UO_2)(AsO_4)](H_2O)_3$, although the latter name has not been

FIG. 15. The interlayer contents of *CsHUAs*, $Cs(H_3O)[(UO_2)(AsO_4)]_2(H_2O)_5$, projected along [001]. Cesium atoms are dark blue large spheres, oxonium groups are pale blue small spheres, and H_2O groups are shown as red spheres. For clarity, only Cs–O bonds and $H_2O...H_3O^+$ interatomic distances are shown.

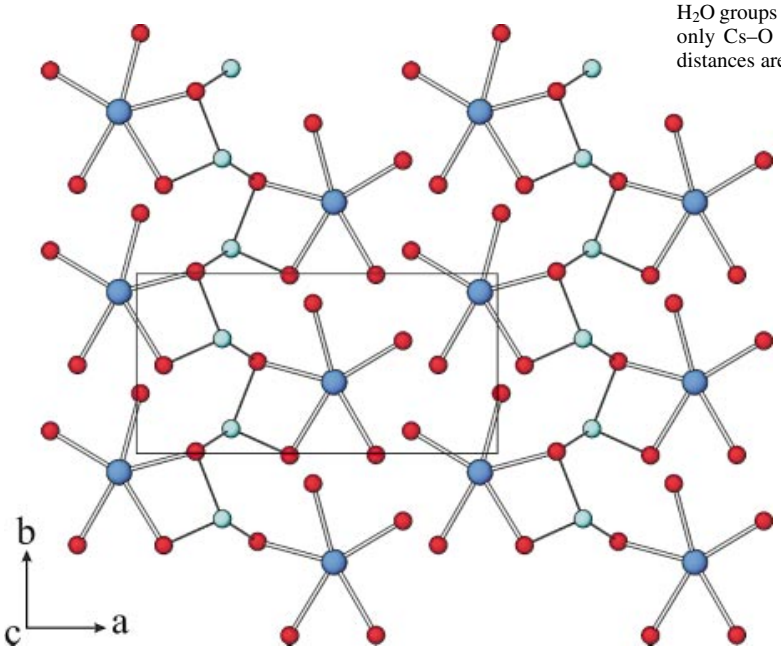

approved by the IMA–CNMMN. Current usage reserves the name sodium uranospinite for the trihydrate (Gaines *et al.* 1997, Anthony *et al.* 2000). The higher hydrates of *NaUP* and *NaUAs* are apparently only transient phases, stable only under very humid conditions or under water (Walenta 1965, Chernikov & Organova 1996); neither has been widely accepted in the literature as a mineral species.

Higher hydrates of *NaUP* and *NaUAs* were not found in the room-temperature syntheses carried out in the context of this work, probably because the hydrolysis of tetramethoxysilane produces methanol as a byproduct, according to the idealized reaction: $(CH_3O)_4Si + 2H_2O = SiO_2 + 4CH_3OH$. The resultant methanol–water mixture in the silica gel has a lower dielectric constant than a purely aqueous solution, and will therefore tend to have lower ionic hydration (Byrappa & Yoshimura 2001), thus favoring the crystallization of the lower hydrates.

The identity of trögerite

Agreement is lacking in the literature on the identity of trögerite, a uranyl arsenate mineral named by Weisbach (1871) from the Walpurgis veins of the Weisser Hirsch mine, Neustädtl, near Schneeburg, Sachsen, Germany, and described as lemon-yellow, tabular monoclinic crystals with density of 3.3 g/cm^3. Goldschmidt (1923) found the mineral to have tetragonal symmetry, based on optical goniometry. Compilations list different chemical formulas for trögerite: *e.g.*, Anthony *et al.* (2000): $(UO_2)_3(AsO_4)_2(H_2O)_{12}$?, Gaines *et al.* (1997): $(H_3O)_2[(UO_2)(AsO_4)]_2(H_2O)_6$? Results of the bulk chemical analyses of trögerite made by Winkler (1873) are not in good agreement with either formula, and Frondel (1958) pointed out that Winkler's analytical data for natural uranospinite, whose U:As ratio is not in doubt, indicated "an almost equally large departure from theory." Weiss *et al.* (1957) presented analyses of a natural uranyl arsenate material with a substantial content of bismuth (7.88 wt% Bi), which has not been accepted in the literature as corresponding to trögerite. Shchipanova *et al.* (1972) described two natural uranyl arsenates: "H-uranospinite", whose chemical composition is in excellent agreement with $(H_3O)[(UO_2)(AsO_4)](H_2O)_3$, and "trögerite", whose composition corresponds only poorly with $(UO_2)_3(AsO_4)_2(H_2O)_{12}$. Natural "hydronium uranospinite" has also been reported from the Jáchymov ore district of the Czech Republic (Ondruš *et al.* 1997).

In this work, we have referred to trögerite as having the composition $(H_3O)[(UO_2)(AsO_4)](H_2O)_3$, consistent with the structures of the meta-autunite group, and isostructural with chernikovite. Compounds with a uranyl to arsenate ratio of 3:2 are not consistent with the stoichiometry and bond-valence requirements of the autunite-type sheet. For example, $(UO_2)_3(AsO_4)_2(H_2O)_5$ and $(UO_2)_3(AsO_4)_2(H_2O)_4$ are framework structures based on the uranophane sheet anion-topology (Locock & Burns 2003d).

On the basis of the report of Shchipanova *et al.* (1972), there may be more than one uranyl arsenate mineral species (devoid of other non-oxonium cations). The IMA Commission on Museums lists cotype trögerite as being held at BAF-Freiberg, Germany. Determination of the identity of trögerite will require care on the part of the investigators. If trögerite corresponds to $(H_3O)[(UO_2)(AsO_4)](H_2O)_3$, this material passes through a phase transition to a lower symmetry structure between 18 and 28°C (de Benyacar & de Abeledo 1974), complicating measurement of its optical and structural properties. Electron-microprobe analysis may prove less than satisfactory because of dehydration and beam-induced mobility of the interlayer cations. Finally, treatment of $(H_3O)[(UO_2)(AsO_4)](H_2O)_3$, whether by grinding to produce a powder, with organic solvents, or by boiling in water, can induce a transformation to poorly crystalline $(UO_2)_3(AsO_4)_2(H_2O)_{12}$ that, upon heating and drying, gives $(UO_2)_3(AsO_4)_2(H_2O)_4$ (Weigel & Hoffmann 1976a, Dorhout *et al.* 1989).

Acknowledgements

This research was supported by the Environmental Management Science Program of the Office of Science, U.S. Department of Energy, grants DE–FGO7–97ER14820 and DE–FGO7–02ER63489. AJL thanks the Environmental Molecular Sciences Institute, University of Notre Dame, for a 2003 EMSI Fellowship, and the International Centre for Diffraction Data for a 2004 Ludo Frevel Crystallography Scholarship. The authors thank Thomas E. Albrecht-Schmitt, Michael E. Zolensky, and the editor, Robert F. Martin, for their comments on the manuscript.

References

Adams, S. (2001): Relationship between bond valence and bond softness of alkali halides and chalcogenides. *Acta Crystallogr.* **B57**, 278-287.

Alberti, A., Fois, E. & Gamba, A. (2003): A molecular dynamics study of the behavior of sodium in low albite. *Am. Mineral.* **88**, 1-10.

Anthony, J.W., Bideaux, R.A., Bladh, K.W. & Nichols, M.C. (2000): *Handbook of Mineralogy*. **IV**. *Arsenates, Phosphates, Vanadates.* Mineral Data Publishing, Tucson, Arizona.

Arend, H. & Connelly, J.J. (1982): Tetramethoxysilane as gel forming agent in crystal growth. *J. Cryst. Growth* **56**, 642-644.

Bean, A.C. & Albrecht-Schmitt, T.E. (2001): Cation effects on the formation of the one-dimensional uranyl iodates $A_2[(UO_2)_3(IO_3)_4O_2]$ (A = K, Rb, Tl) and AE $[(UO_2)_2$

$(IO_3)_2O_2]$ (H_2O) (*AE* = Sr, Ba, Pb). *J. Solid State Chem.* **161**, 416-423.

BEINTEMA, J. (1938): On the composition and crystallography of autunite and the meta-autunites. *Recl. Trav. Chim. Pays-Bas* **57**, 155-175.

BENAVENTE, J., RAMOS BARRADO, J.R., CABEZA, A., BRUQUE, S. & MARTINEZ, M. (1995): A comparative study of the electrical behaviour of different uranyl phosphate-based membranes by a.c. and d.c. measurements. *Colloids Surf. A* **97**, 13-20.

BERGERIOUX, C., KENNEDY, G. & ZIKOVOSKY, L. (1979): Use of the semi-absolute method in neutron activation analysis. *J. Radioanal. Chem., Articles* **50**, 229.

BOTTO, I.L., BARAN, E.J. & AYMONINO, P.J. (1975): Kristallographische Daten von Ammoniumuranylphosphattrihydrat. *Z. Chemie* **16**, 163.

BROWN, I.D. & ALTERMATT, D. (1985): Bond-valence parameters obtained from a systematic analysis of the inorganic crystal structure database. *Acta Crystallogr.* **B41**, 244-247.

BRUKER-AXS (1998): *SAINT, V 5.01 program for reduction of data collected on Bruker AXS CCD area detector systems.* Bruker Analytical X-ray Systems, Madison, Wisconsin.

BUCK, E.C., BROWN, N.R., & DIETZ, N.L. (1996): Contaminant uranium phases and leaching at the Fernald site in Ohio. *Environ. Sci. Technol.* **30**, 81-88.

BURNS, P.C. (1999): The crystal chemistry of uranium. *In* Uranium: Mineralogy, Geochemistry and the Environment (P.C. Burns & R. Finch, eds.). *Rev. Mineral.* **38**, 23-90.

_____, EWING, R.C. & HAWTHORNE, F.C. (1997): The crystal chemistry of hexavalent uranium: polyhedron geometries, bond-valence parameters, and polymerization of polyhedra. *Can. Mineral.* **35**, 1551-1570.

BUTT, C.R.M. & GRAHAM, J. (1981): Sodian potassian hydroxonian meta-autunite: first occurrence of an intermediate member of a predicted solid solution series. *Am. Mineral.* **66**, 1068-1072.

BYRAPPA, K. & YOSHIMURA, M. (2001): *Handbook of Hydrothermal Technology.* Noyes Publications, Park Ridge, N.J.

CANDEA, R.M., LUPU, D., CHIRTOC, M., DADARLAT, D. & FRANDAS, A. (1993): Pyroelectric spectroscopy of the hydrogen uranyl phosphate. *Spectrosc. Lett.* **26**, 923-934.

CASCIOLA, M. (1996): Ionic conductivity in layered materials. *In* Solid-State Supramolecular Chemistry: Two- and Three-Dimensional Inorganic Networks (G. Alberti & T. Bein, eds.). Elsevier Science, New York, N.Y. (355-378).

CHERNIKOV, A.A. & ORGANOVA, N.I. (1996): Natroautunite and metanatroautunite. *Dokl. Acad. Sci., Earth Sci. Sect.* **341A**, 109-113.

CHERNORUKOV, N.G., KARYAKIN, N.V., SULEIMANOV, E.V. & CHERNORUKOV, G.N. (1994a): Preparation and characterization of $A(I)PUO_6{\bullet}nH_2O$ compounds. *Radiochemistry* (transl. of *Radiokhimiya*) **36**, 227-232.

_____, _____, _____ & _____ (1994b): Synthesis and investigation of $M^IAsUO_6{\bullet}nH_2O$ compounds. *Russ. J. Inorg. Chem.* (transl. of *Zh. Neorg. Khim.*) **39**, 20-23.

_____, SULEIMANOV, E.V. & ERMONIN, S.A. (2001): Structure and thermodynamics of solid solutions $HP_{1-x}As_x$ $UO_6{\bullet}4H_2O$. *Russ. J. Gen. Chem.* **71**, 491-494.

_____, _____ & _____ (2002): Isomorphism in alkali metal uranophosphates $APUO_6{\bullet}nH_2O$. *Russ. J. Gen. Chem.* **72**, 161-164.

_____, _____ & NIPRUK, O.V. (2003): Heterogeneous equilibria in the systems uranophosphate $A^IPUO_6{\bullet}nH_2O$–aqueous solution (A^I = H, Li, Na, K, Rb, Cs). *Radiochemistry* (transl. of *Radiokhimiya*) **45**, 117-121.

CHILDS, P.E., HALSTEAD, T.K., HOWE, A.T. & SHILTON, M.G. (1978): N.M.R. study of hydrogen motion in hydrogen uranyl phosphate (HUP) and hydrogen uranyl arsenate (HUAs). *Mat. Res. Bull.* **13**, 609-619.

_____, HOWE, A.T. & SHILTON, M.G. (1980): Studies of layered uranium(VI) compounds. V. Mechanisms of densification of hydrogen uranyl phosphate tetrahydrate (HUP): pressure-induced planar glide and solution phase sintering. *J. Solid State Chem.* **34**, 341-346.

COLE, M., FITCH, A.N. & PRINCE, E. (1993): Low-temperature structure of $KUO_2PO_4{\bullet}3D_2O$ determined from combined synchrotron radiation and neutron powder diffraction measurements. *J. Mater. Chem.* **3**, 519-522.

COTTON, F.A., WILKINSON, G., MURILLO, C.A. & BOCHMANN, M. (1999): *Advanced Inorganic Chemistry* (6th ed.). John Wiley & Sons, New York, N.Y.

DE BENYACAR, M.A.R. & DE ABELEDO, M.E.J. (1974): Phase transition in synthetic troegerite at room temperature. *Am. Mineral.* **59**, 763-767.

_____ & DUSSEL, H.L. (1975): Ferroelectricity and phase transitions in $H_2(UO_2)_2(AsO_4)_2{\bullet}8H_2O$. *Ferroelectrics* **9**, 241-244.

_____ & _____ (1978): Symmetry and phase transitions in $(AsO_4)_2H_2(UO_2)_2{\bullet}8H_2O$. *Ferroelectrics* **17**, 469-472.

DIECKMANN, G.H. & ELLIS, A.B. (1987): Interlamellar Liebig titration based on photoluminescence. Reaction of silver uranyl phosphate with hydrogen cyanide gas. *Inorg. Chem.* **26**, 4147-4148.

DORHOUT, P.K., ROSENTHAL, G.L. & ELLIS, A.B. (1989): Two families of lamellar, luminescent solid solutions: the intercalative conversion of hydrogen uranyl phosphate arsenates to uranyl phosphate arsenates. *Solid State Ionics* **32/33**, 50-56.

DUSSEL, H.L., DE WAINER, L.S. & DE BENYACAR, M.A.R. (1982): Ferroelasticity in phase II of synthetic troegerite. *Ferroelectrics* **46**, 25-31.

FAIRCHILD, J.G. (1929): Base exchange in artificial autunites. *Am. Mineral.* **14**, 265-275.

FINCH, R. & MURAKAMI, T. (1999): Systematics and paragenesis of uranium minerals. *In* Uranium: Mineralogy, Geochemistry and the Environment (P.C. Burns & R. Finch, eds.). *Rev. Mineral.* **38**, 91-180.

FISCHER, R., GERT-DIETER, W., LEHMANN, T, HOFFMANN, G. & WEIGEL, F. (1981): The phosphates and arsenates of hexavalent actinides. IV. Plutonium. *J. Less Common Metals* **80**, 121-132.

FITCH, A.N., BERNARD, L., HOWE, A.T., WRIGHT, A.F. & FENDER, B.E.F. (1983): The room-temperature structure of $DUO_2AsO_4{\bullet}4D_2O$ by powder neutron diffraction. *Acta Crystallogr.* **C39**, 159-162.

_____ & COLE, M. (1991): The structure of $KUO_2PO_4{\bullet}3D_2O$ refined from neutron and synchrotron-radiation powder diffraction data. *Mat. Res. Bull.* **26**, 407-414.

_____ & FENDER, B.E.F. (1983): The structure of deuterated ammonium uranyl phosphate trihydrate, $ND_4UO_2PO_4{\bullet}3D_2O$, by powder neutron diffraction. *Acta Crystallogr.* **C39**, 162-166.

_____, _____ & WRIGHT, A.F. (1982a): The structure of deuterated lithium uranyl arsenate tetrahydrate $LiUO_2AsO_4{\bullet}4D_2O$ by powder neutron diffraction. *Acta Crystallogr.* **B38**, 1108-1112.

_____, WRIGHT, A.F. & FENDER, B.E.F. (1982b): The structure of $UO_2DAsO_4{\bullet}4D_2O$ at 4 K by powder neutron diffraction. *Acta Crystallogr.* **B38**, 2546-2554.

FRONDEL, C. (1958): Systematic mineralogy of uranium and thorium. *U.S. Geol. Surv., Bull.* **1064**.

GAINES, R.V., SKINNER, H.C.W., FOORD, E.E., MASON, B. & ROSENZWEIG, A. (1997): *Dana's New Mineralogy* (8th ed.). John Wiley & Sons, New York, N.Y.

GARCIA, F.G. & DIAZ, R.R. (1959a): Constitution and physicochemical properties of some uranyl double phosphates and analogous substances. I. Synthesis and chemical composition. *Anales real soc. espan. fis y. quim.* (*Madrid*) **55B**, 383-398.

_____ & _____ (1959b): Constitution and physicochemical properties of some uranyl double phosphates and analogous substances. II. Ion-exchange properties. *Anales real soc. espan. fis y. quim.* (*Madrid*) **55B**, 399-406.

_____ & _____ (1962): Structure and physical-chemical properties of some double phosphates of uranyl and analogous substances. *Acta Salamant. Cienc.* **5**, 523-531.

GOLDSCHMIDT, V. (1923): *Atlas der Krystallformen* IX. Facsimile Reprint, 1986, Rochester Mineralogical Symposium, Rochester, N.Y.

GRAHAM, J., BUTT, C.R.M. & VIGERS, R.B.W. (1984): Subsurface charging, a source of error in microprobe analysis. *X-ray Spectrom.* **13**, 126-133.

GROAT, L.A., JAMBOR, J.L. & PEMBERTON, B.C. (2003): The crystal structure of argentojarosite, $AgFe_3(SO_4)_2(OH)_6$. *Can. Mineral.* **41**, 921-928.

HAWTHORNE, F.C. (1997): Structural aspects of oxide and oxysalt minerals. *In* Modular Aspects of Minerals (S. Merlino, ed.). *Eur. Mineral. Union, Notes in Mineralogy* **1**, 373-429.

_____, UNGARETTI, L. & OBERTI, R. (1995): Site populations in minerals: terminology and presentation of results of crystal structure refinement. *Can. Mineral.* **33**, 907-911.

HENISCH, H.K. (1988): *Crystals in Gels and Liesegang Rings.* Cambridge University Press, New York, N.Y.

HERBST-IRMER R. & SHELDRICK, G.M. (1998): Refinement of twinned structures with *SHELXL97*. *Acta Crystallogr.* **B54**, 443-449.

IBERS, J.A. & HAMILTON, W.C., eds. (1974): *International Tables for X-ray Crystallography* **IV.** The Kynoch Press, Birmingham, U.K.

JAMESON, G.B. (1982): On structure refinement using data from a twinned crystal. *Acta Crystallogr.* **A38**, 817-820.

JEFFREY, G.A. (1997): *An Introduction to Hydrogen Bonding*. Oxford University Press, New York, N.Y.

JOHNSON, C.M., SHILTON, M.G. & HOWE, A.T. (1981): Studies of layered uranium(VI) compounds. VI. Ionic conductivities and thermal stabilities of $MUO_2PO_4{\bullet}nH_2O$, where M = H, Li, Na, K, NH_4 or ½ Ca, and where n is between 0 and 4. *J. Solid State Chem.* **37**, 37-43.

KARYAKIN, N.V., CHERNORUKOV, N.G., SULEIMANOV, E.V. & MOCHALOV, L.A. (1999): Thermodynamics of compounds of the $A^IB^VUO_6{\bullet}H_2O$ series. Heat capacity and thermodynamic functions of uranophosphates A^IPUO_6 (A^I = H, Li, Na, K, Rb, Cs). *Russ. J. Gen. Chem.* **69**, 8-10.

KREUER, K.-D. (1996): Proton conductivity: materials and applications. *Chem. Mater.* **8**, 610-641.

KRIVOVICHEV, S.V. & BROWN, I.D. (2001): Are the compressive effects of encapsulation an artifact of the bond valence parameters? *Z. Kristallogr.* **216**, 245-247.

LEIGH, G.J., ed. (1990): *Nomenclature of Inorganic Chemistry: Recommendations 1990*. International Union of Pure and Applied Chemistry, Commission on the Nomenclature of Inorganic Chemistry. Blackwell Scientific Publications, London, U.K.

LOCOCK, A.J. & BURNS, P.C. (2002) Crystal structures of three framework alkali metal uranyl phosphate hydrates. *J. Solid State Chem.* **167**, 226-236.

_____ & _____ (2003a): Crystal structures and synthesis of the copper-dominant members of the autunite and meta-autunite groups: torbernite, zeunerite, metatorbernite and metazeunerite. *Can. Mineral.* **41**, 489-502.

_____ & _____ (2003b): Revised Tl(I)–O bond valence parameters and the structures of thallous dichromate and thallous uranyl phosphate hydrate. *Z. Kristallogr.* **219**, 259-266.

_____ & _____ (2003c): Structures and synthesis of framework Rb and Cs uranyl arsenates and their relationships with their phosphate analogues. *J. Solid State Chem.* **175**, 372-379.

_____ & _____ (2003d): Structures and syntheses of framework triuranyl diarsenate hydrates. *J. Solid State Chem.* **176**, 18-26.

LUPU, D., GRECU, R. & BIRIŞ, A.R. (1993): Polaron effects in the protonic conductor hydrogen uranyl phosphate. *Phys. Stat. Sol.* **B178**, 281-288.

MACASKIE, L.E., BONTHRONE, K.M., YONG, P. & GODDARD, D.T. (2000): Enzymically mediated bioprecipitation of uranium by a *Citrobacter* sp.: a concerted role for exocellular lipopolysaccharide and associated phosphatase in biomineral formation. *Microbiology* **146**, 1855-1867.

_____, EMPSON, R.M., CHEETHAM, A.K., GREY, C.P. & SKARNULISS, A.J. (1992): Uranium bioaccumulation by a *Citrobacter* sp. as a result of enzymically mediated growth of polycrystalline HUO_2PO_4. *Science* **257**, 782-784.

MAGALHÃES, M.C.F., DE JESUS, J.D.P. & WILLIAMS, P.A. (1985): The chemistry of uranium dispersion in groundwaters at the Pinhal do Souto mine, Portugal. *Inorg. Chim. Acta* **109**, 71-78.

MANGHI, E. & POLLA, G. (1983): Hydrogen uranyl arsenate hydrate single crystals: $H_2(UO_2)_2(AsO_4)_2•8H_2O$; gel growth and characterization. *J. Cryst. Growth* **61**, 606-614.

MARKOVIĆ, M., PAVKOVIĆ, N. & PAVKOVIĆ, N. D. (1988): Precipitation of $NH_4UO_2PO_4•3H_2O$ – solubility and structural comparison with alkali uranyl(2+) phosphates. *J. Res. Natl. Bur. Stand.* **93**, 557-563.

METCALFE, K., HALSTEAD, T.K. & SLADE, R.C.T. (1988): NMR studies of hydrogen diffusion in hydrogen uranyl phosphate tetrahydrate (HUP). *Solid State Ionics* **26**, 209-215.

MOROSIN, B. (1978a): Structural mechanism for H+ ion conductivity in HUP. *Phys. Lett. A* **65**, 53-54.

_____ (1978b): Hydrogen uranyl phosphate tetrahydrate, a hydrogen ion solid electrolyte. *Acta Crystallogr.* **B34**, 3732-3734.

MURAKAMI, T., OHNUKI, T., ISOBE, H. & TSUTOMU, T. (1997): Mobility of uranium during weathering. *Am. Mineral.* **82**, 888-899.

ONDRUŠ, P., VESELOVSKÝ, F., SKÁLA, R., CÍSAŘOVÁ, I., HLOUŠEK, J., FRÝDA, J., VAVŘÍN, I.,ČEJKA, J. & GABAŠOVÁ, A. (1997): New naturally occurring phases of secondary origin from Jachymov (Joachimstahl). *J. Czech Geol. Soc.* **42**, 77-108.

PEARSON, R.G. (1993): Chemical hardness – a historical introduction. *Struct. Bonding* **80**, 2-10.

PERRINO, C.T. & LEMASTER, C.B. (1984): Preparation of $HUO_2PO_4•4H_2O$ single crystals from gel. *J. Cryst. Growth* **69**, 639-640.

PHAM-THI, M. & COLOMBAN, P. (1985): Cationic conductivity, water species motions and phase transitions in $H_3OUO_2PO_4•3H_2O$ (HUP) and MUP related compounds ($M^+ = Na^+$, K^+, Ag^+, Li^+, NH_4^+). *Solid State Ionics* **17**, 295-306.

_____, _____ & NOVAK, A. (1985): Vibrational study of $H_3OUO_2PO_4•3H_2O$ (HUP) and related compounds. Phase transitions and conductivity mechanisms. I. $KUO_2PO_4•3H_2O$ (KUP). *J. Phys. Chem. Solids* **46**, 493-504.

POINSIGNON, C. (1989): The use of quasielastic neutron scattering to study the mechanism of proton transfer in fast solid protonic conductors. *Solid State Ionics* **35**, 107-113.

PUZIEWICZ, J. (1995): Sodium meta-autunite,* sodium autunite. *Am. Mineral.* **80**, 1329-1330.

RENNINGER, N., MCMAHON, K.D., KNOPP, R., NITSCHE, H., CLARK, D.S. & KEASLING, J.D. (2001): Uranyl precipitation by biomass from an enhanced biological phosphorus removal reactor. *Biodegradation* **12**, 401-410.

ROBERT, M.C. & LEFAUCHEUX, F. (1988): Crystal growth in gels: principle and applications. *J. Cryst. Growth* **90**, 358-367.

ROH, Y., LEE, S.R., CHOI, S.K., ELLESS, M.P. & LEE, S.Y. (2000): Physicochemical and mineralogical characterization of uranium contaminated soils. *Soil and Sediment Contamination* **9**, 463-486.

ROSS, M. & EVANS, H.T., JR. (1964): Studies of the torbernite minerals. I. The crystal structure of abernathyite and the structurally related compounds $NH_4(UO_2AsO_4)•3H_2O$ and $K(H_3O)(UO_2AsO_4)_2•6H_2O$. *Am. Mineral.* **49**, 1578-1602.

_____ & _____ (1965): Studies of the torbernite minerals. III. Role of the interlayer oxonium, potassium, and ammonium ions, and water molecules. *Am. Mineral.* **50**, 1-12.

ROSS, V. (1955): Studies of uranium minerals. XXI. Synthetic hydrogen-autunite. *Am. Mineral.* **40**, 917-919.

SCHULTE, E. (1965): Zur Kenntnis der Uranglimmer. *Neues Jahrb. Mineral., Monatsh.*, 242-246.

SHANNON, R.D. (1976): Revised effective ionic radii and systematic studies of interatomic distances in halides and chalcogenides. *Acta Crystallogr.* **A32**, 751-767.

SHCHIPANOVA, O.V., BELOVA, L.N., PRIBYTKOV, P.V. & KATARGINA, A.P. (1972): New data on the structure and identification of trögerite and hydrogen-uranospinite. *Dokl. Akad. Nauk SSSR* **197**, 109-111 (in Russ.).

SHELDRICK, G.M. (1998): *SHELXTL NT, V5.1 Program Suite for Solution and Refinement of Crystal Structures*. Bruker Analytical X-ray Systems, Madison, Wisconsin.

SHILTON, M.G. & HOWE, A.T. (1979): Hydrogen-bond ordering in the proton conductors hydrogen uranyl phosphate and arsenate tetrahydrates. *J. Chem. Soc. Chem. Comm*., 194-196.

SMITH, D.K. (1984): Uranium mineralogy. *In* Uranium Geochemistry, Mineralogy, Geology, Exploration and Resources (B. De Vivo, F. Ippolito, G. Capaldi & P.R. Simpson, eds.). Institute of Mining and Metallurgy, London, U.K. (43-88).

SOWDER, A.G., CLARK, S.B. & FJELD, R.A. (1996): The effect of silica and phosphate on the transformation of schoepite to becquerelite and other uranyl phases. *Radiochim. Acta* **74**, 45-49.

SULEIMANOV, E.V., CHERNORUKOV, N.G., KARYAKIN, N.V. & ERMILOV, S.E. (2002a): Thermodynamics of dehydration of $A^IPUO_6 \cdot xH_2O$ (A^I = Li, Na, K, Rb, Cs) crystal hydrates. *Radiochemistry* (transl. of *Radiokhimiya*) **44**, 452-457.

_____, KARYAKIN, N.V. & ERMILOV, S.E. (2002b): Systems A^IPUO_6–H_2O (A^I = Na, K): phase diagrams and thermochemistry. *Russ. J. Gen. Chem.* **72**, 1160-1163.

VAN HAVERBEKE, L., VOCHTEN, R. & VAN SPRINGEL, K. (1996): Solubility and spectrochemical characteristics of synthetic chernikovite and meta-ankoleite. *Mineral. Mag.* **60**, 759-766.

VESELÝ, V., PEKÁREK, V. & ABBRENT, M. (1965): A study on uranyl phosphates. III. Solubility products of uranyl hydrogen phosphate, uranyl orthophosphate and some alkali uranyl phosphates. *J. Inorg. Nucl. Chem.* **27**, 1159-1166.

VOCHTEN, R. (1990): Transformation of chernikovite and sodium autunite into lehnerite. *Am. Mineral.* **75**, 221-225.

WALENTA, K. (1965): Die Uranglimmergruppe. *Chem. Erde* **24**, 254-278.

WEIGEL, F. & HOFFMANN, G. (1976a): The phosphates and arsenates of hexavalent actinides. I. Uranium. *J. Less Common Metals* **44**, 99-123.

_____ & _____ (1976b): The phosphates and arsenates of hexavalent actinides. II. Neptunium. *J. Less Common Metals* **44**, 125-132.

_____ & _____ (1976c): The phosphates and arsenates of hexavalent actinides. III. Ammonium americyl (VI)-phosphate. *J. Less Common Metals* **44**, 133-136.

WEISBACH, A. (1871): Vorläufige Mitteilung – Trögerit, Walpurgin. *Neues Jahrb. Mineral.*, 869-870.

WEISS, A., TABORSZKY, F., HARTL, K. & TRÖGER, E. (1957): Zur Kenntnis des Uranminerals Trögerit. *Z. Naturforsch.* **12b**, 356-358.

WELLMAN, D.M. & ICENHOWER, J.P. (2002): Direct synthesis of Na-autunite. *Geochim. Cosmochim. Acta* **66**, Suppl. 1, A828.

WINKLER, C. (1873): Ueber die chemische Constitution einiger neuer Uranmineralien. *J. prakt. Chemie* **7**, 1-14.

ZOLENSKY, M.E. (1983): *The Structures and Crystal Chemistry of the Autunite and Meta-autunite Mineral Groups. Appendix* **1**, *Gel Growth Experiments*. Ph.D. thesis, Pennsylvania State Univ., University Park, Pennsylvania, U.S.A.

Received January 29, 2004, revised manuscript accepted May 4, 2004.